The 3rd Generation Synchrotron Light Sources

Shunqiang TIAN, SSRF, SARI, CAS

Sep. 9, 2025, Shanghai, PRC

SSRF 上海同步辐射光源 Shanghai Synchrotron Radiation facility

Outline

- The Way to the 3rd GLS
- Progress in the 3rd GLS
- Overview of SSRF
- Beam Dynamics in SSRF
- Summary

Outline

- The Way to the 3rd GLS
- Progress in the 3rd GLS
- Overview of SSRF
- Beam Dynamics in SSRF
- Summary

Synchrotron Radiation and Facilities

◆ **The first artificial synchrotron radiation**

- In 1947, a kind of artificial electromagnetic radiation was **observed** in a 70 MeV synchrotron of the General Electric Corporation, which is the origin of its name Synchrotron Radiation.

- Tracking back history, synchrotron radiation was **predicted** by Lienard et. al. at the end of 19th century. A charged particle will emitt electromagnetic radiation, when its equilibrium state is changed. For a circulating particle moving in a speed of relativity, its radiation concentrates in a very narrow angle around its moving direction.

- Synchrotron radiation was **validated** before its first observation by measurements of electron orbit change in a 100 MeV Betatron.

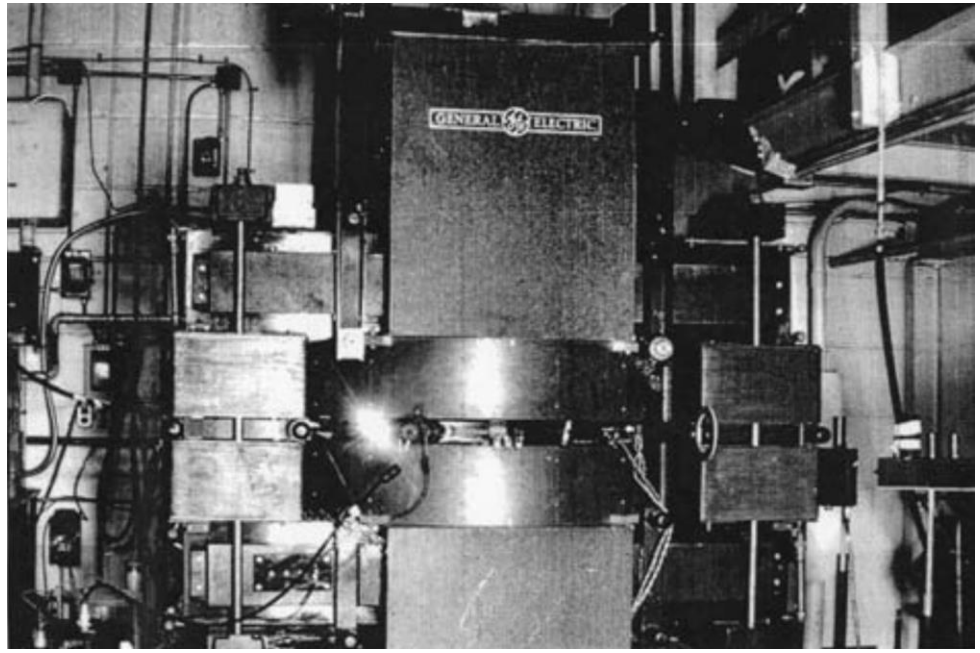

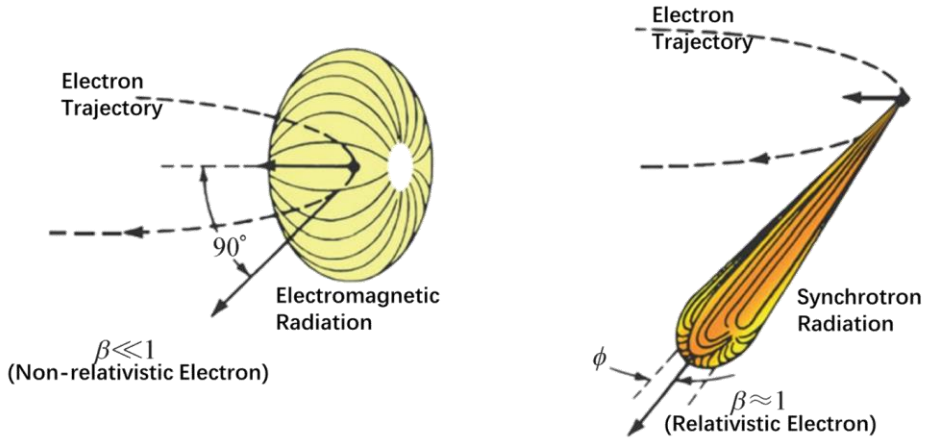

◆ Synchrotron radiation application

- Synchrotron radiation is the main obstacle of particle's acceleration in high energy, while its **unique properties**, high brilliance, continuous spectra, high stability, accurate predictablitiy, granted the great-potential application in the studies of the electronic and optical charateristics of solids liquids and gases.
- The applications started from Vacuum UltraViolet, and soon expanded to X-ray.
- The photons' phenomenons of **tansimission scattering and obsorption/excitation** were took as an powerful investigator to implement imagning, structure/ingredient analysis, and spectroscopy in physics chemistry and biology.

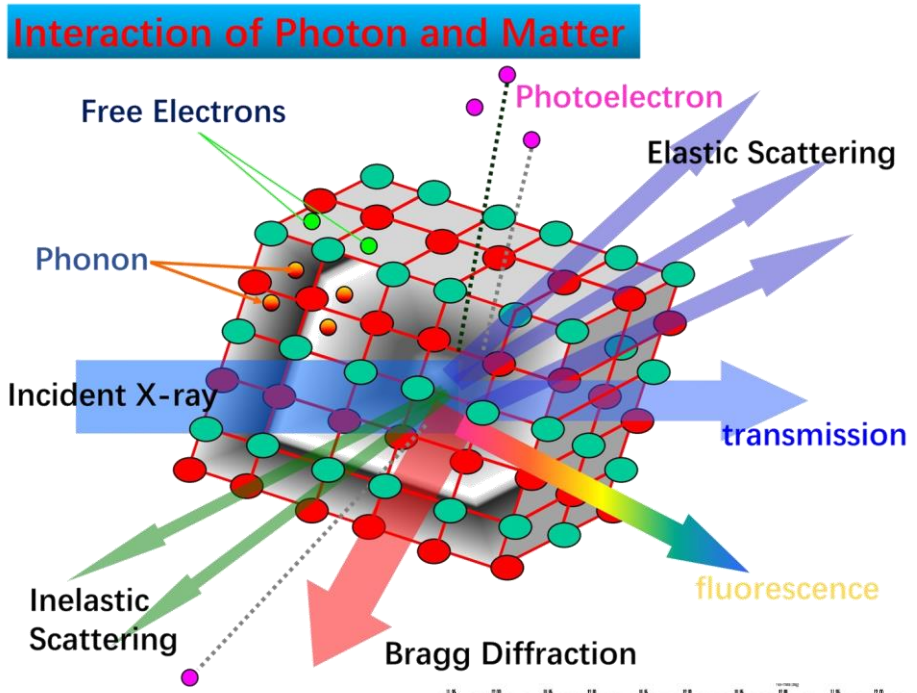

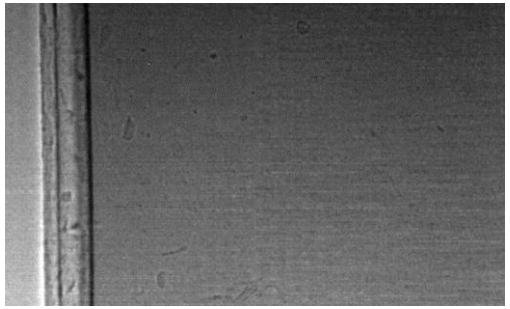

Fast dynamic process imaging

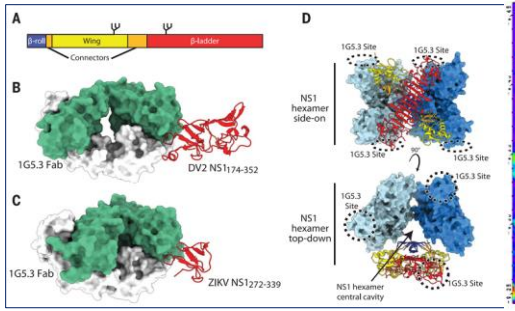

Structural analysis of antibody-virus complex

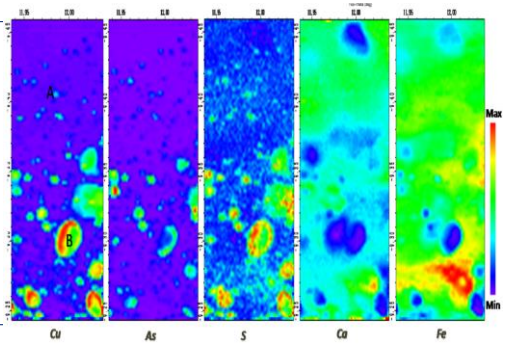

Ingredient analysis in ceramic cross-section

◆ Synchrotron radiation facilities

- The 1st generation light sources: parasitic in high energy colliders
- The 2nd generation light sources: dedicated storage rings, mainly use photons emitted from dipoles. The **developments of insertion devices and Chasman-Green lattice** paved the way to the 3rd GLS.
- The 3rd generation light sources: featured by low emittance based on C-G lattice, and higher flux and brilliance from IDs.
- The 4th generation light sources: by pushing beam emittance down to X-ray diffraction limit, delivering high-spatically coherent and ultimate-highly bright photons.

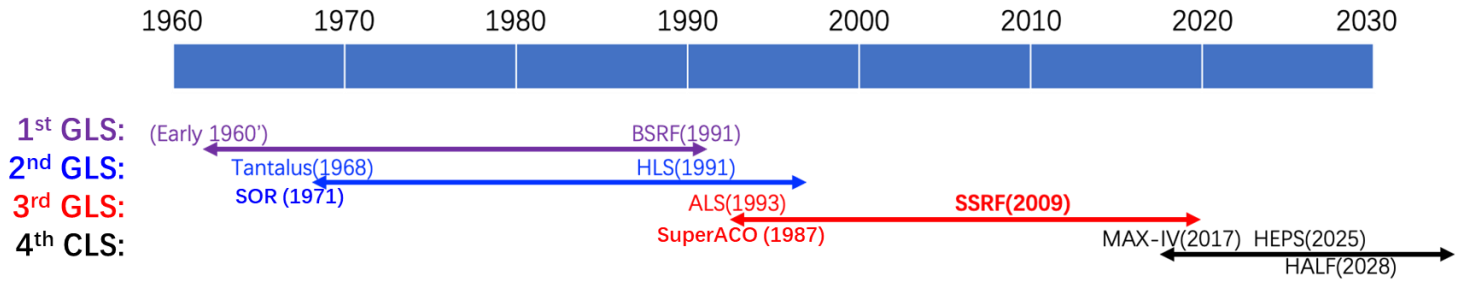

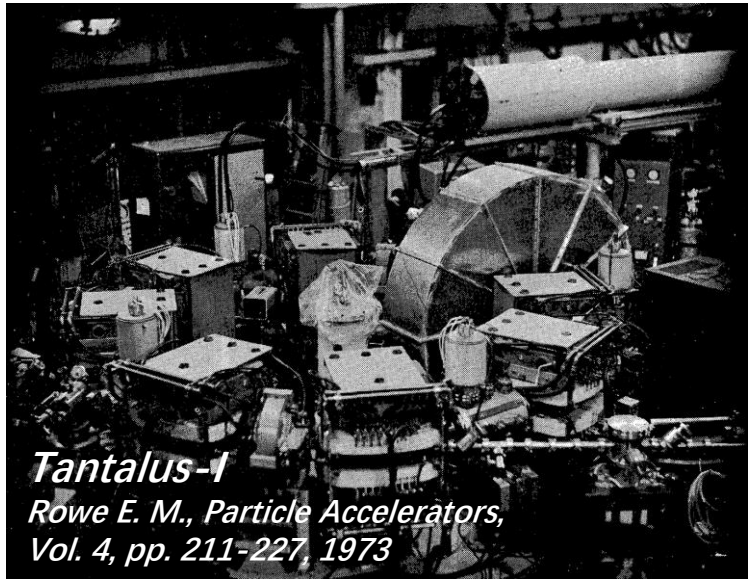

Invention of Insertion Device

- **The first ID in synchrotron light souce**

- **Wiggler:** served as a synchrotron source first at SLAC and BINP in 1978, while it was electrical-magnetic type.

- **Undulator:** permanent-magnetic type, manufactured in SLAC in 1980.

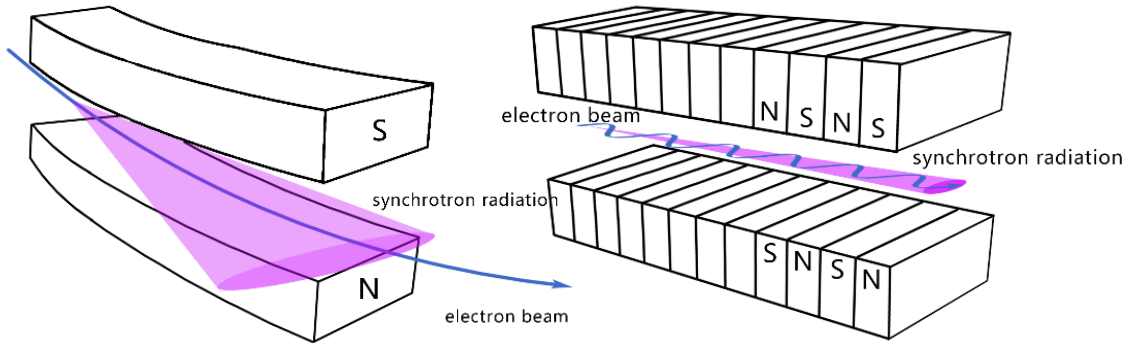

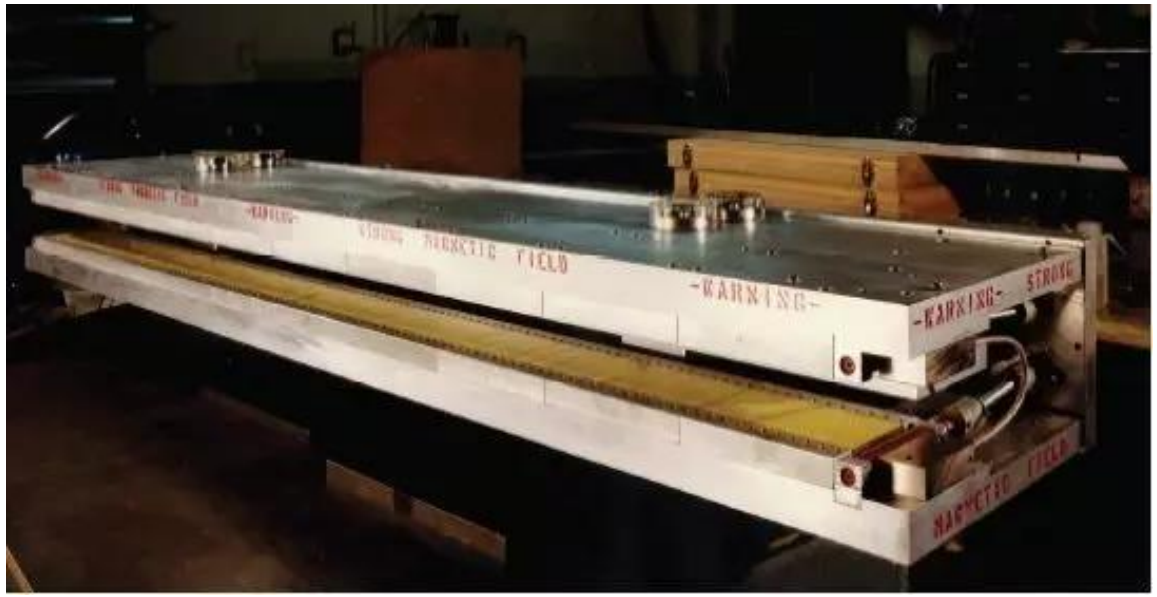

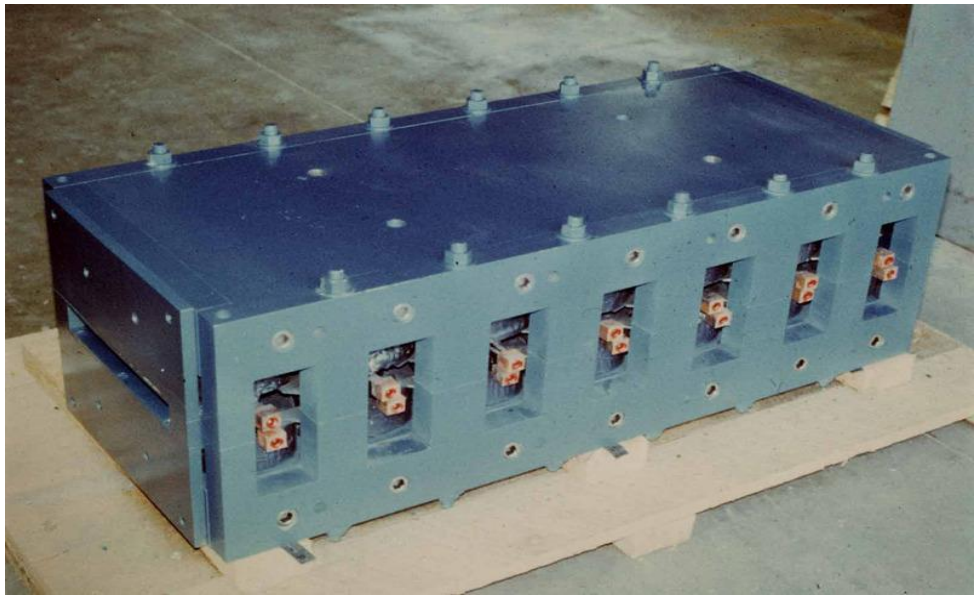

➢ Strength parameter:

$$K = \frac{eB_0}{\beta m_e c k_\mathrm{p}} = \gamma\vartheta = 93.4\, B\lambda_\mathrm{p}$$

- A periodic magnetic field device is called undulator if K≤1 (small amplitude and high frequency of electron oscilation in ID), and a wiggler if K >>1 (large amplitude and low frequency).

➢ Spectra:

- Photon spectra from a wiggler is a continuous curve, just like from a dipole, while the spectra from a undulator is a series of peaks whose energy can vary in a range by adjusting its gap (or peak field).

- More theoritically, the wiggler also emitt line spectra. However, the high-energy peaks are close enough to merge to a curve, because of the non-zero peak width.

- **Generally, undulator is used to provide highly bright photons, wihle wiggler is applied to generate high flux of photons.**

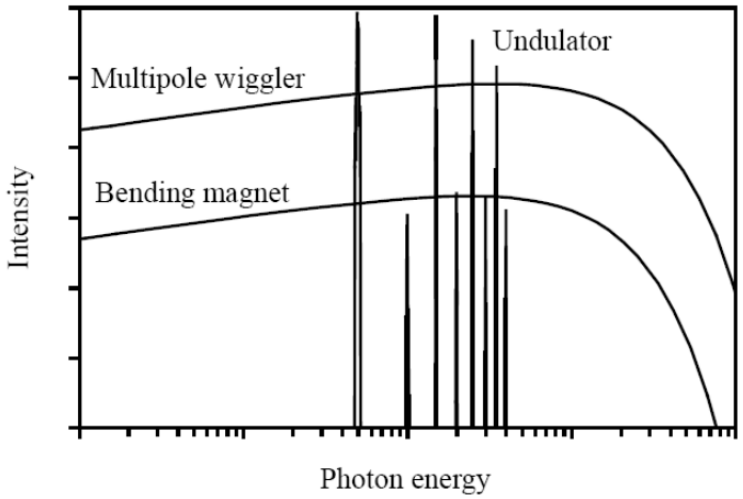

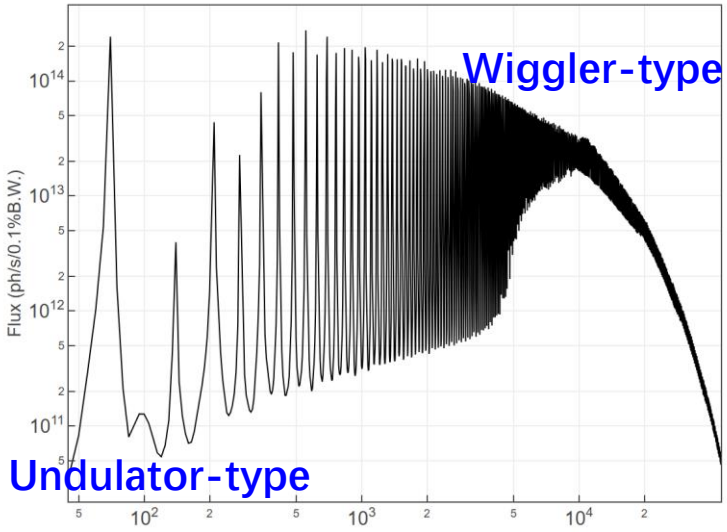

Chasman-Green Lattice and TME

◆ Chasman-Green Lattice

- In 1975, Chasman and Green designed a dedicated storage ring for synchrotron facility, which incorporated with high field superconducting wigglers serving as hard radiation ports and made available a wide spectrum for simultaneous experiments.

- The lattice consists of six arcs matched to six straight sections. Each arc consists of two achromatic bends separated by a Q-triplet.

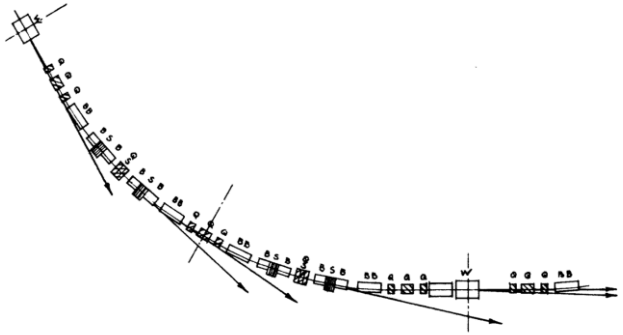

- The most important and remarkable factors were the lattice includes six **straight sections** specifically for installing IDs, and **low-beta and free-dispersion** are matched for IDs to increase the photon brilliance and suppress IDs' impacts on beam dynamics.

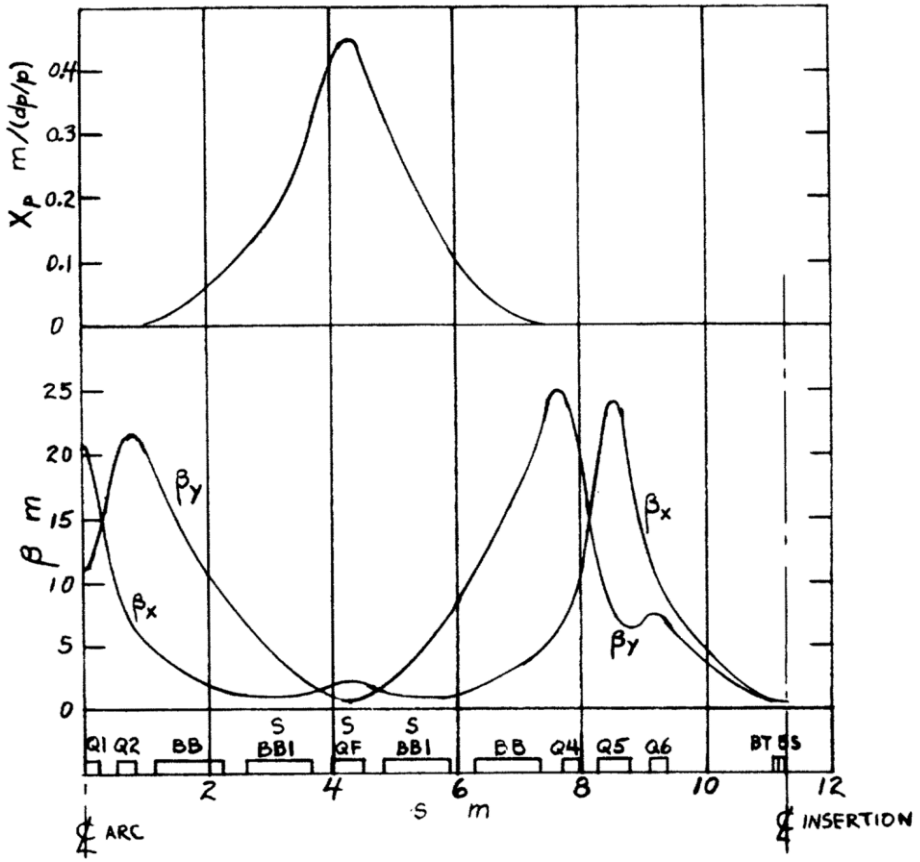

Chasman R., Green G. K., Rowe E. M., Transactions on Nuclear Science, Vol. NS-22, No. 3, 1765-1768, 1975

◆ Double-Bend Achromatic (DBA) lattice

- The CG structure is slightly inflexible and the lattice chromaticity is not easily controllable by sextupoles in the locations available for them.
- DBA (modified from C-G lattice) replaces the B-Q triplets between achromatic dipoles with Q-doublets, leaving enough space for sextupoles and creating adequate β-separation for chromaticity correction. **More familiar to the later learners**
- This modification greatly improves the flexibility for adjusting the lattice functions in dipoles approaching lower emittance, whilst maintaining low-β and zero-dispersion in the straight sections.
- DBA is the most frequently encountered lattice amongst the 2nd and 3rd GLS.

NSLS-VUV ring as an example

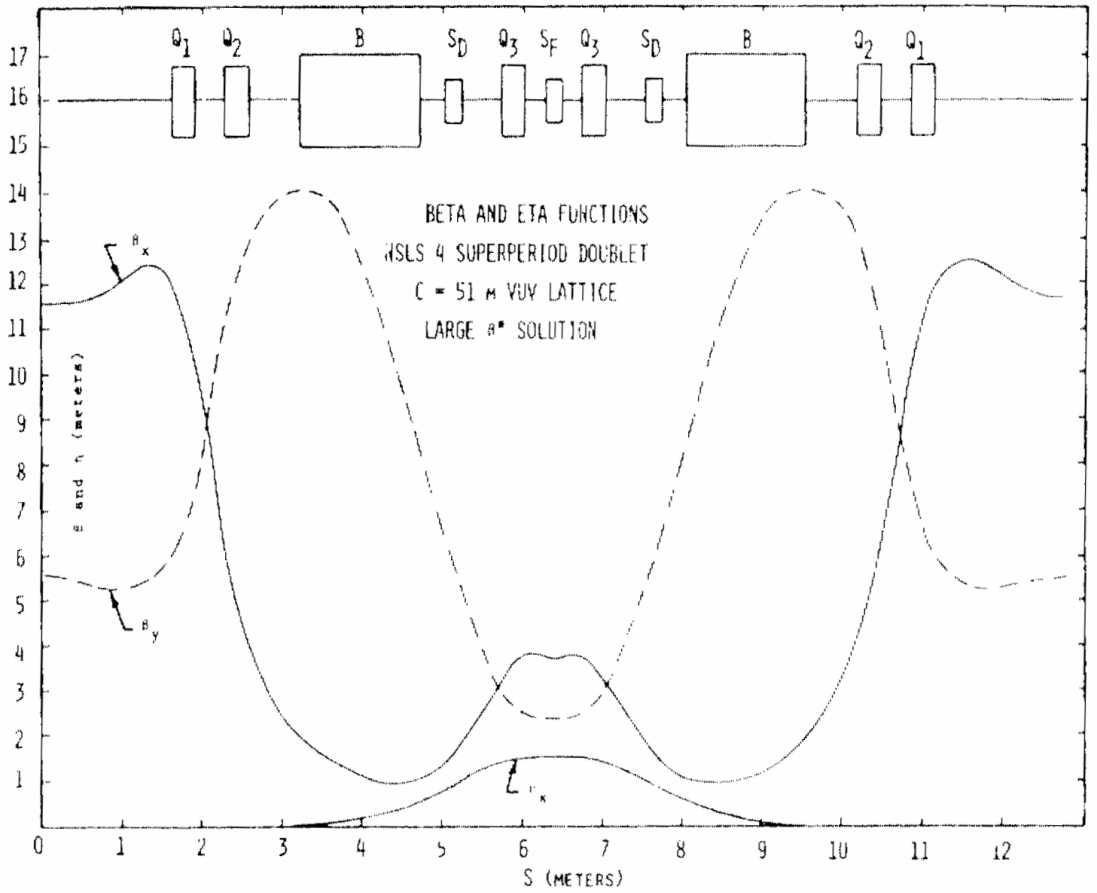

Blumberg L. et. al., IEEE Transactions on Nuclear Science, Vol. NS-26, No. 3, 1979

◆ Theoritical Minimum Emittance (TME)

➢ The natural emittance is determined by equilibrium state between quantum excitation and radiation damping.

$$\varepsilon_x = \frac{C_q \gamma_s^2}{J_x} \frac{\langle (1/\rho)^3 \mathcal{H} \rangle}{\langle (1/\rho)^2 \rangle} \qquad \mathcal{H} = \frac{1}{\beta}\left[\eta^2 + \left(\beta\eta' - \frac{1}{2}\beta'\eta\right)^2\right] \qquad J_x = 1 - \mathcal{D} \qquad \mathcal{D} = \frac{\oint \eta(1+2\rho^2 K) ds/\rho^3}{\oint ds/\rho^2}$$

➢ Considering constant field dipole, a terse equation with ***<H>***:

$$\varepsilon_x = \frac{C_q \gamma_s^2}{J_x \rho} \langle \mathcal{H} \rangle$$

$$\begin{aligned} \langle \mathcal{H} \rangle &= \gamma_0 \eta_0^2 + 2\alpha_0 \eta_0 \eta_0' + \beta_0 \eta_0'^2 + (\alpha_0 \eta_0' + \beta_0 \eta_0') \frac{L}{\rho} \\ &+ \left(\frac{\beta_0}{3\rho^2} - \frac{\alpha_0 \eta_0'}{3\rho} - \frac{\gamma_0 \eta_0}{3\rho}\right) L^2 - \frac{\alpha_0 L^3}{4\rho^2} + \frac{\gamma_0 L^4}{20\rho^2} \end{aligned}$$

Twiss transport in dipoles:

$$\begin{aligned} \beta(s) &= \beta_0 - 2\alpha_0 s + \gamma_0 s^2 \\ \alpha(s) &= \alpha_0 - \gamma_0 s \\ \gamma(s) &= \gamma_0 \\ \eta(s) &= \eta_0 + \eta_0' s + \rho(1 - \cos(s/\rho)) \\ \eta'(s) &= \eta_0' + \sin(s/\rho) \end{aligned}$$

➢ When $\frac{\partial \langle \mathcal{H} \rangle}{\partial \beta_0} = 0, \frac{\partial \langle \mathcal{H} \rangle}{\partial \alpha_0} = 0, \frac{\partial \langle \mathcal{H} \rangle}{\partial \eta_0} = 0, \frac{\partial \langle \mathcal{H} \rangle}{\partial \eta_0'} = 0$, and its second derivatives large than 0, the TME is got.

Teng L. C., Argonne National Laboratory, LS-17, 1985

- Achromatic dipole

  η_0 and η_0' at then entrance of dipole are zero,

$$\eta_0 = 0, \eta_0' = 0, \frac{\partial\langle\mathcal{H}\rangle}{\partial\beta_0} = 0, \frac{\partial\langle\mathcal{H}\rangle}{\partial\alpha_0} = 0$$

  Solve the above eqution, result in that when β reaches minimum value at 3L/8 away from dipole's entrance, the natural emittance reaches its TME.

$$\beta_{x,TME,Achro.} = \frac{3}{8\sqrt{15}}L$$

$$\varepsilon_{x,TME,Achro.} = \frac{C_q\gamma^2}{J_x}\frac{\theta^3}{4\sqrt{15}}$$

- Chromatic dipole (assume β and η reach minimum in the centre of Diople)

$$\alpha_0|_{L/2} = 0, \eta_0'|_{L/2} = 0, \frac{\partial\langle\mathcal{H}\rangle}{\partial\beta_0} = 0, \frac{\partial\langle\mathcal{H}\rangle}{\partial\eta_0} = 0$$

$$\beta_{x,TME,Chro.} = \frac{1}{2\sqrt{15}}L, \eta_{TME,Chro.} = \frac{L^2}{24\rho}$$

$$\varepsilon_{x,TME,Chro.} = \frac{C_q\gamma^2}{J_x}\frac{\theta^3}{12\sqrt{15}}$$

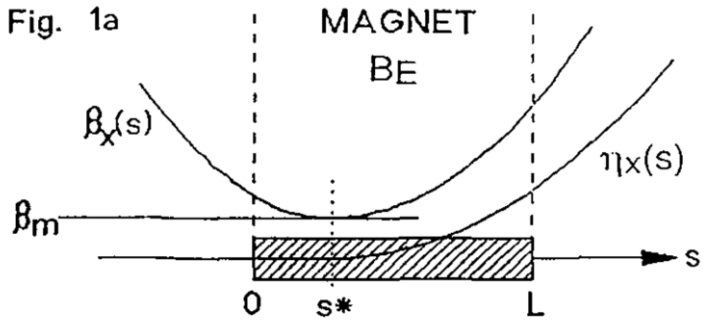

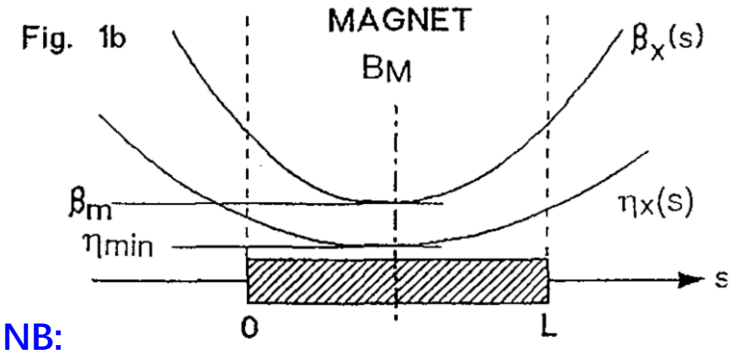

NB:

- Mechanism of minimizing emittance is reducing the quantum excitation by optimizing H function in dipoles.
- TME is proportional to θ^3 that is the reason of sharp emittance reduction in MBA lattice. It is also made by weakening the quantum excitation.

Construction of the 3rd GLSs

◆ **The first cluster of the 3rd GLSs**

- VUV source **Super-ACO**, operated in 1987, is the earliest explorer of the 3rd GLSs that was designed from the start with low emittance, and to accomodate several insertion devices (eight straight sections, six for IDs, and four dispersion-free sections).

- In the research of atomic/molecular/surface science, and condensed matter physics, materials science, the solution to a series of scientific problems relied on highly-intense extreme ultraviolet (EUV) and hard X-ray. **Low-energy and high-energy light sources** had been successfully constructed and operated in Western Europe, North America, and East Asia, in 1990s'.

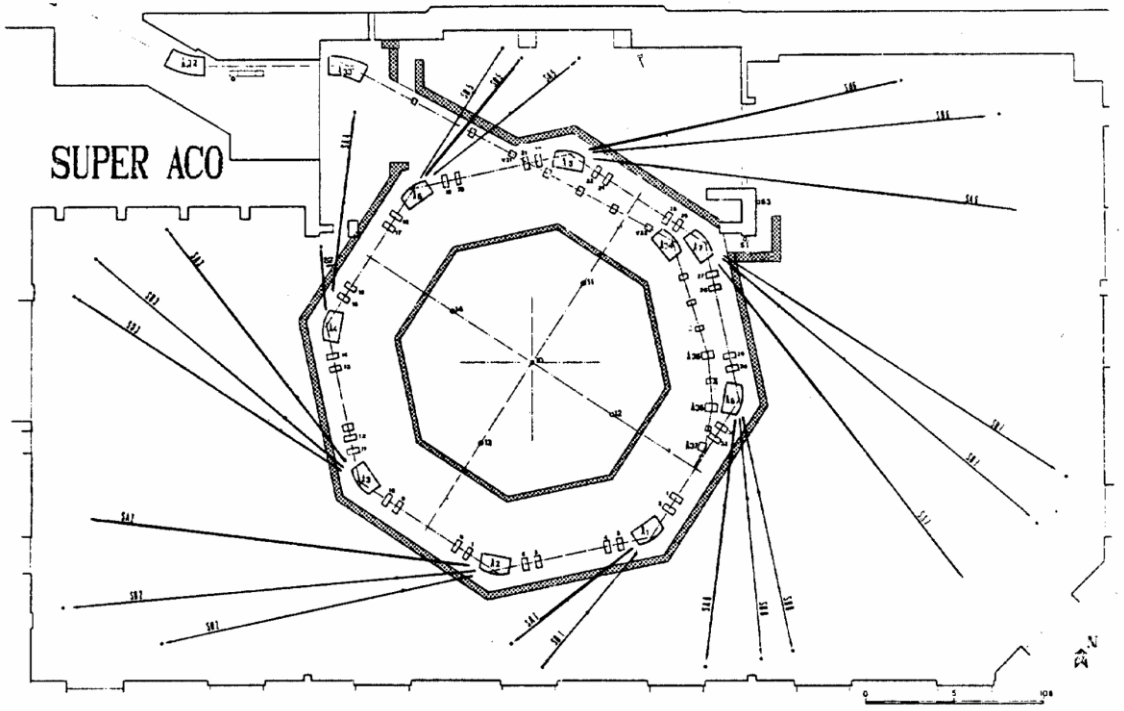

Beam energy: 800 MeV,
Beam emittance: ~30 nm.rad
Ring circumference: 72 m
Beam current: 500 mA
Number of light ports: 13 (Dipole)
6 (Undulator)

➢ A summery of the 3rd GLSs built in 1990s'

- Large capacity for IDs: the ratios of straight section are 20%~40%.
- Length of straight ~6 m for different kinds of IDs.
- Natural emittance reached lower than 10 nm.rad.

Name	E_0/ GeV	C_0/ m	$\varepsilon_{N,x}$ / nm.rad	I_0 / mA	Straight / m	Site	Year
ESRF	6.0	844.4	4.0	200	32 X 6.3	Grenoble	1994
APS	7.0	1104	3.0	100	40 X 5.8	Argonne	1996
Spring-8	8.0	1436	2.8	100	44 X 6.6 4 X 30.0	Hyogo	1997
ALS	1.9	196.8	2.1	400	12 X 6.7	Berkeley	1993
Elettra	2.0/2.4	259.0	7.0	300	12 X 6.1	Trieste	1994
TLS	1.5	120.0	22	360	6 X 6.0	Hsinchu	1994
PLS	2.0	280.6	12	200	12 X 6.8	Pohang	1994
MAX-II	1.5	90.0	8.8	280	10 X 3.1	Lund	1996
BESSY-II	1.7	240	6.1	200	8 X 5.7 8 X 4.9	Berlin	1999

◆ The medium-energy light sources

- In the late 1990s', life science, environment science, and energy science had made great innovations, and the demands for synchrotron radiation were increased. The interested photon spectra was **X-ray from 3 to 30 keV**.

- Combined developed IDs, the medium-energy **(E_0~3.0GeV)** facilities were the best platforms to provide high flux and brilliance of X-ray from 3~30 keV.

- The first 3rd generation medium-energy light source is Swiss Light Source (2001), followed by ANKA (2002) CLS (2003) and SPEAR3 (2003).

- The medium-energy light sources have high cost-effectiveness. With the optimal soft X-ray, their spectra still fully cover the range from infrared (Dipole-edge) to hard X-rays (SCW).

◆ World distribution of the 3rd GLSs

- More than 20 3rd-GLS facilities are in routinely operation all over the world.
- The dense aeras include East Asia, West Europe, and North America.
- ESRF APS SPring8, and ALS SLS Elettra had been or were being upgraded to the 4th GLSs.
- Most of all the other 3rd GLSs had their upgrade proposals that apply MBA lattice to reduce the emittance down to X-ray diffraction limits.

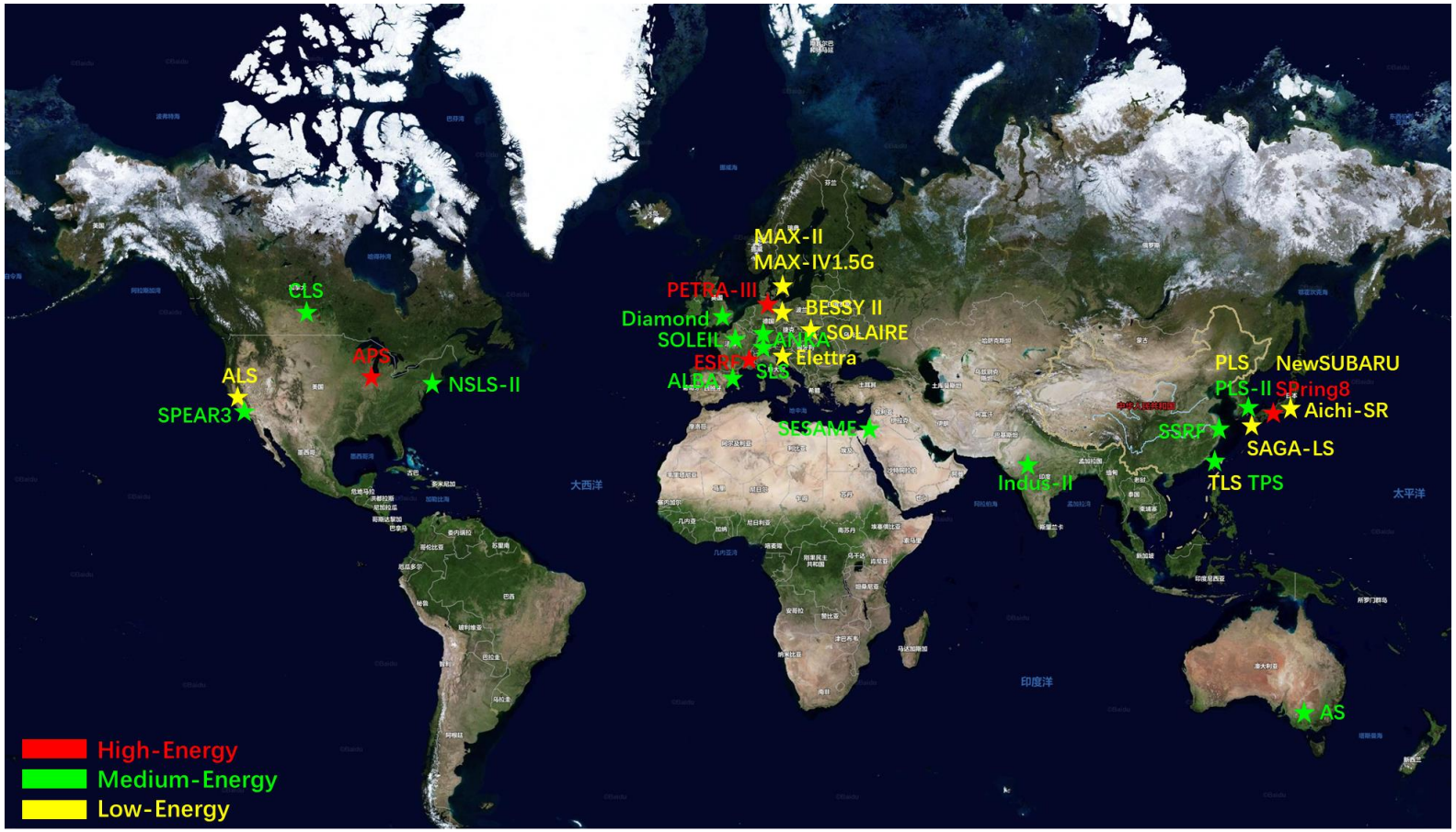

Outline

- The Way to the 3rd GLS
- **Progress in the 3rd GLS**
- Overview of SSRF
- Beam Dynamics in SSRF
- Summary

Nonlinear Optimization

◆ Harmonic sextupoles

- To reduce the beam emittance, DBA and TBA lattices apply very strong focusing gradient, resulting in high chromaticities. The sextupoles are used to correct chromaticities, while it nonlinearize the particle motion leading to not enough dynamic aperture or energy acceptance.

- An effective method is install extra sextupoles in zero-/low-dispersion sections (harmonic sextupole) to cancel aberrations of the particle motion. Example: Diamond DBA, SLS TBA.

- From the start of lattice design, nonlinear opitimization, tangled with linear optics design, is a painstaking work.

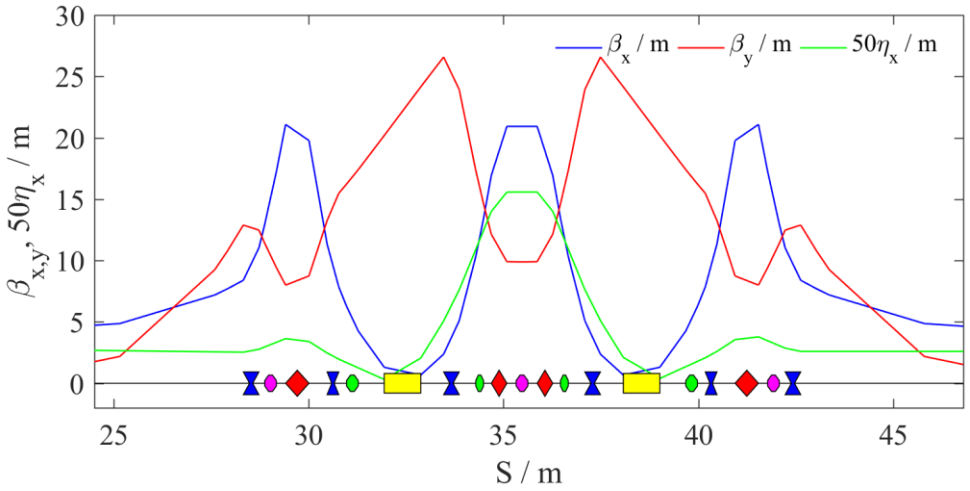

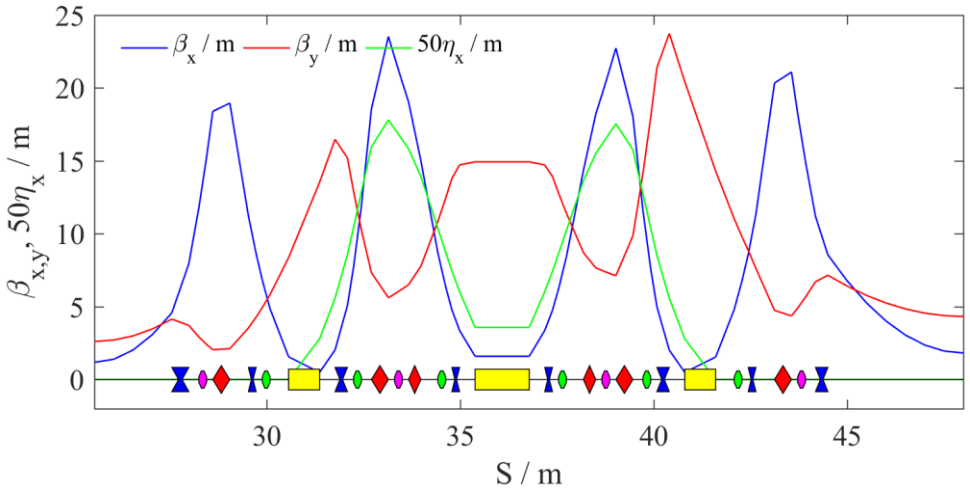

◆ Nonliear driving terms

- Descriped in **perturbation theory**, the particle motion consists of fundamental mode and a series of geometric and chromatic aberrations.
- If the aberrations can be reduce sufficiently that means particle motion is linearized enough, and dynamic acceptance can be easily increased.
- The first order nonlinear aberrations are most harmful to the lattice performance.
- All the parameters in equations are linear optics and gradient integrals, so caculating the driving terms is very fast.
- The SLS as an example showing the effects of harmonic sextupoles.

$$h_3 = \sum_J h_{jklmp} (2J_x)^{(j+k)/2} (2J_y)^{(l+m)/2} \delta^p + \ldots$$

$$h_{jklmp} = h^*_{kjmlp} =$$

$$\sum_n^{N_{sext}} (b_3 L)_n \beta_{xn}^{\frac{(j+k)}{2}} \beta_{yn}^{\frac{(l+m)}{2}} \eta_n^p e^{i[(j-k)\varphi_{xn}+(l-m)\varphi_{yn}]} - \left[\sum_n^{N_{quad}} (b_2 L)_n \beta_{xn}^{\frac{(j+k)}{2}} \beta_{yn}^{\frac{(l+m)}{2}} e^{i[(j-k)\varphi_{xn}+(l-m)\varphi_{yn}]} \right]_{p\neq 0}$$

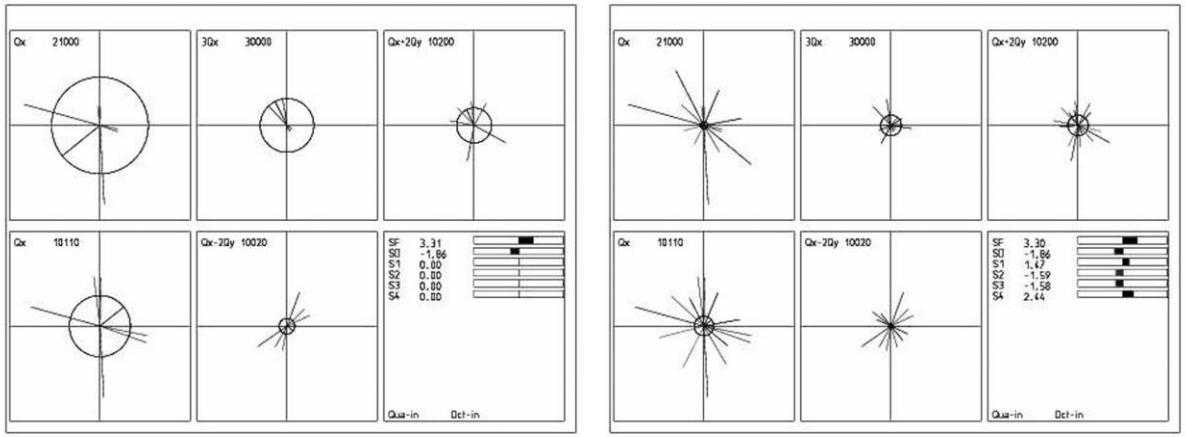

- The circles show vector sum of sextupoles in one cell.
- The left plot is only SD and SF, while the right plot show the results with harmonic sextupoles. Cancellation in one cell is remarkable.

Streun A., in proceedings of CERN Accelerator School, 203, 2006
Bengtsson J., SLS Note 9/97

◆ Frequency Map Analysis (FMA)

- FMA was introduced in accelerator physics by J. Laskar, in early 1990s'. It was first applied in the ALS storag ring.

- In a conservative system, the motion in phase space takes place on tori, which are described by either Action (J) or Frequency (ν). A one-to-one maps can be built.

$$Maps: J \rightarrow \upsilon$$

- If the system becomes non-integrable because of nonlineare perturbation, there is no smooth tori exsiting or the motion takes place in random/chaotic layer (resonance).

$$z = A_w e^{i\nu_w t} + \sum_{k=1}^{N} A_k e^{i(m_k,\nu)t}$$

- In this case, stable J/ν cannot be found. The diffusion rate with turns/time is applied to measure the instability.

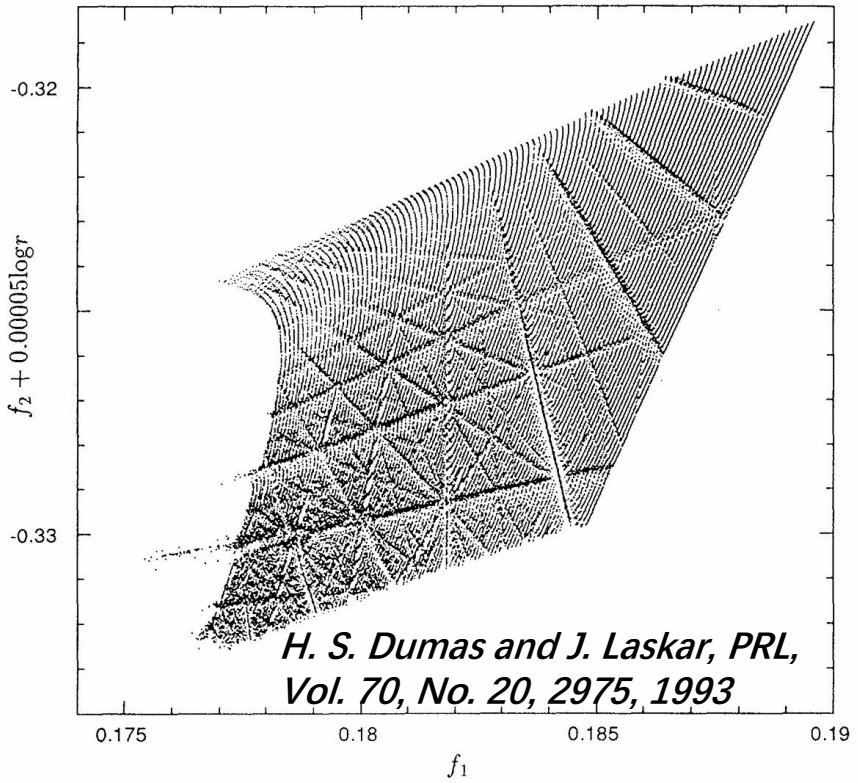

H. S. Dumas and J. Laskar, PRL, Vol. 70, No. 20, 2975, 1993

$$D = lg\sqrt{(\upsilon_x^1 - \upsilon_x^2)^2 - (\upsilon_y^1 - \upsilon_y^2)^2}$$

- We use frequency, because it is easy sampled and highly precise with the method of NAFF.

- ALS as an example: FMA shows all the nonlinear resonances (and their relative strenghth and width), resonance nodes, islands, and folds in DA and FM.

- The new information can help nonlinear optimization in the storage ring. Guide the designer to find a stable working point, increase DAs, enhance the robust of the lattice performance to magnetic errors (prevent any occurance of maps' fold, strong resonances and their nodes).

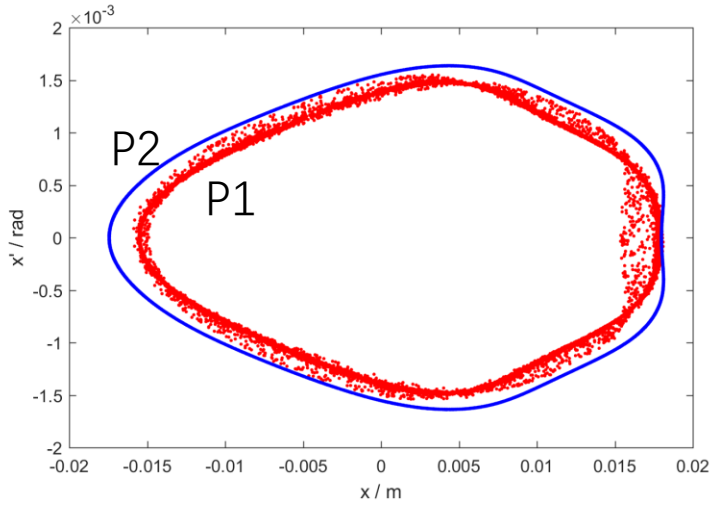

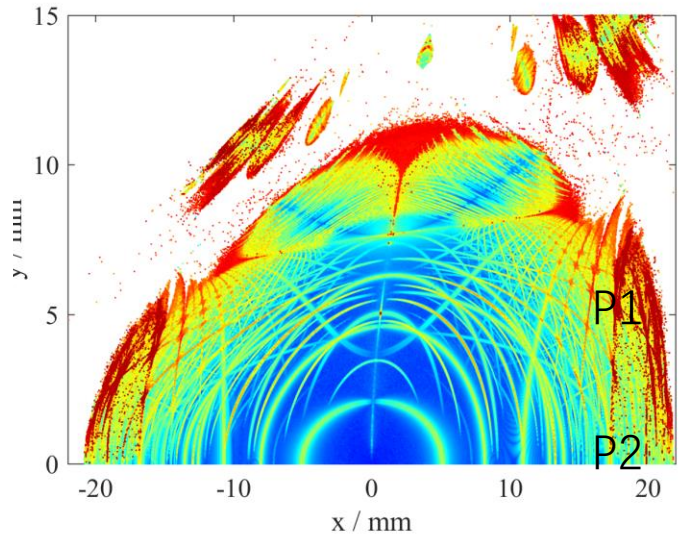

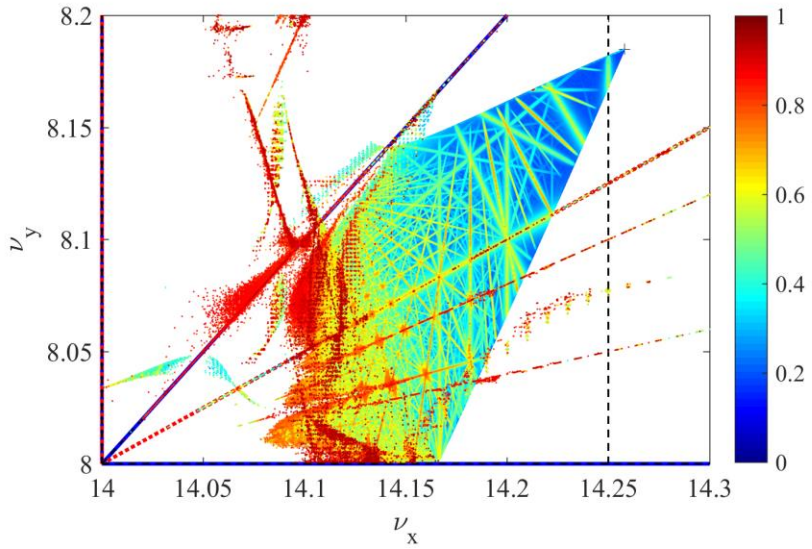

◆ Multi-objective bionical algorithm application

- Design and optimization for storage rings is a typical multi-objective and multi-knob problem.
- Non-dominant sorting of multi objectives to find the optimal-front (Pareto-front) enables a global optimization of the beam optics and dynamics, facilitating to obtain the best solution.
- The **Pareto-front** is defined as a cluster of solutions, where there is no other solution whose all the objectives are prior to those solutions.
- The objectives are usually chosen two or more conflict properties/parameters, such as emittance and DA, EA and DA, working point and emittance, and so on.
- Algorithms:
  Genetic-Algorithems, Particle Swarm Optimization, etc.

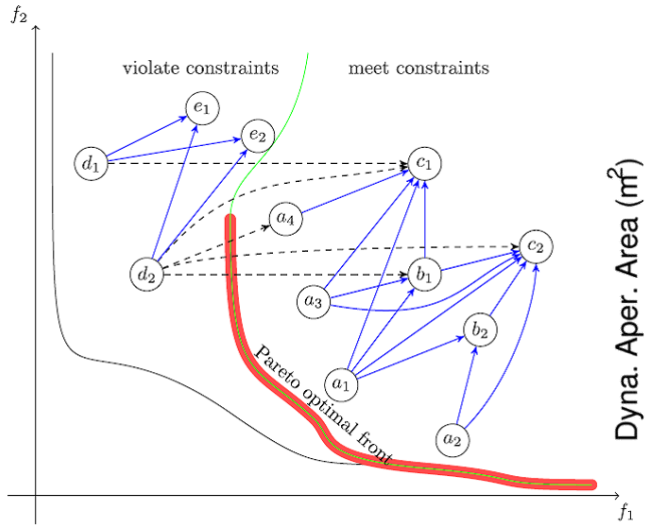

Non-dominated sorting for multiobjective optimization problems with constraints (case of two objective functions minimized). The arrow shows *dominance*, and dashed lines are broken dominance due to constraints.

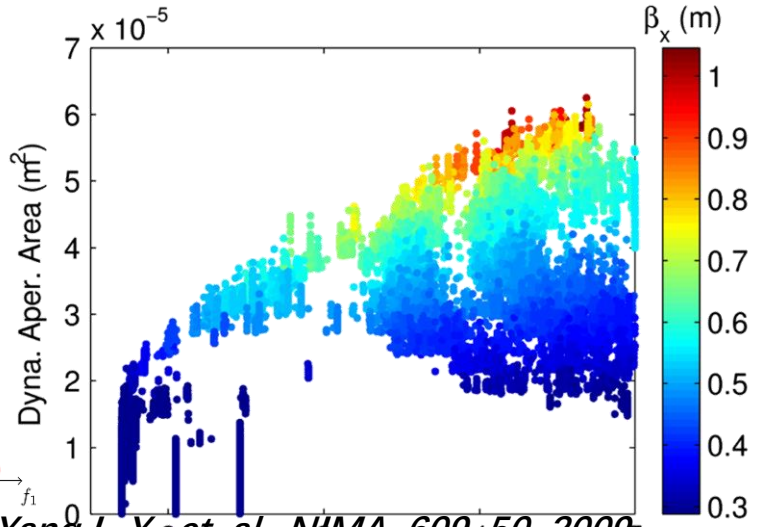

Yang L. Y.et. al., NIMA, 609,50, 2009
Sun C. C., et. al., PRST-A&B, 15, 054001, 2012

◆ A summary of nonlinear optimization methods

➢ The basic process of nonlinear optimization is that appling descent algorithm to adjust the possible knobs, reaching the best objectives.

Knob	Objective	Algorithm
Periodicity, Symmetry	Driving Terms	Gauss-Newton Algorithm
Linear Optics	Action-Angle Variable	L-M Decent Method
Phase Advance in Sextupole	Approximation of linearity	Conjugate Method, Powell Method
Harmonic Sextupole	Tracked DA/EA	Genetic Algorithm
Pi-Track	Tracked FMA	Particle Swarm Optimization
Octupole	Parameter Predictd by ML	Machine Learning
……	……	……

Beam Dynamics

◆ Vertical emittance control

- Vertical emittance originates from betatron coupling and verticle dispersion.
- Brilliance: $$B(\lambda, t, x, y) = \delta(t)\Delta(t, x, y)\frac{Flux(\lambda)}{\varepsilon_x \varepsilon_y}$$
- ASP used LOCO method and mechanical alignments to successfully correct the vertical emittance down to about 1.30 pm.rad that is well below the hard X-ray diffraction limits.
- Side effects of ultralow vertical emittance include strong intra-beam scattering, and Touschek scattering. (However, they were not severe in ASP case.)
- A conservative criterion is correcting ε_y below ~50 pm.rad in low- and medium-energy facilities, ~5 pm.rad in high-energy facilities, reaching diffraction limits of their optimal spectra.

Vertical dispersion reduction

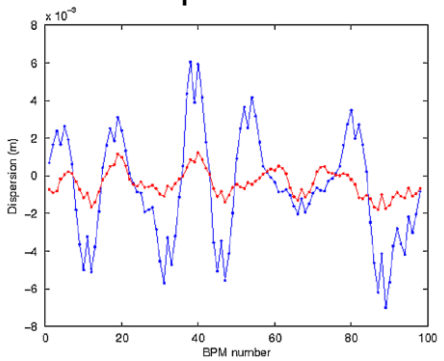

Corrected betatron coupling

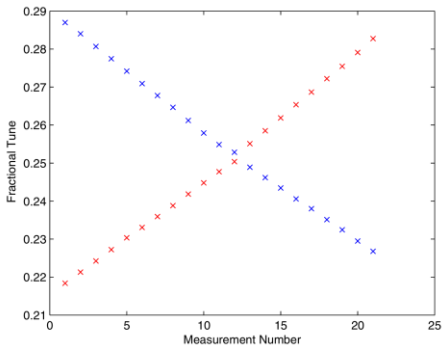

ε_y~1 pm.rad κ~0.01%

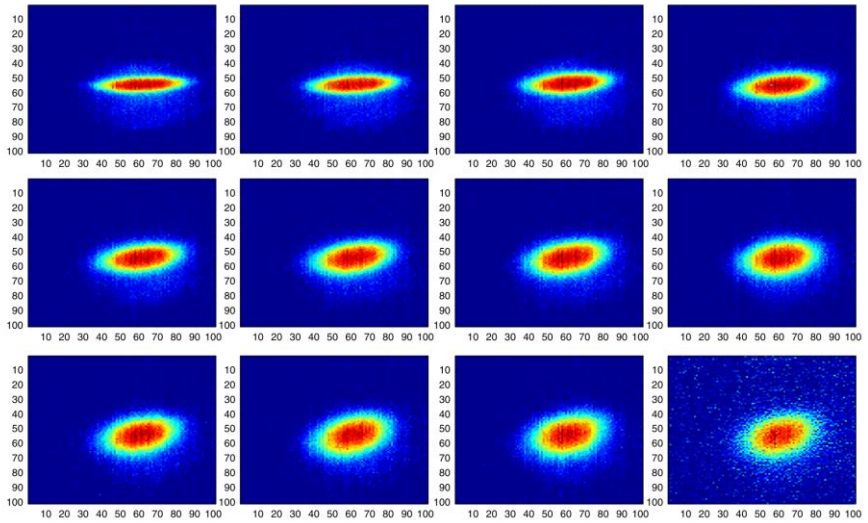

ε_y~100 pm.rad

R. Dowd, et. al., PRST-A&B, 14, 012804, 2011

◆ Collective effects

- Beam collective effects concerned in the 3rd GLSs, including head-tail instability, Transverse Mode Coupling Instability, microwave instability, and coupled bunch instability, had been recognized and well studied during 1960s' to 1980s'. With assistance of bunch lengthening and transverse feedback, and a delicate impedance budget, the maximum beam current in the 3rd GLSs reached 500 mA.

- In 1997, a new kind of beam instability, **Fast Beam-Ion Instability**, was observed in the ALS storage ring, by artificially increasing vaccum pressure.

- Transient ions induced by highly-intense electron bunch accumulate in the path along the bunch train. The tail bunches are easy to oscilate coupled by ions. FBII is likely to occur in new rings and linacs.

- The cure method of FBII is vaccume clearing, and shortening the bunch train.

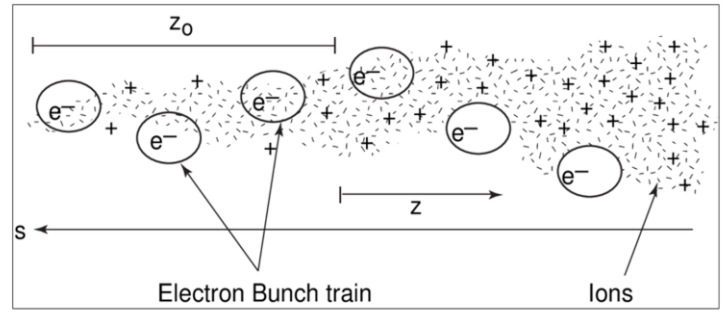

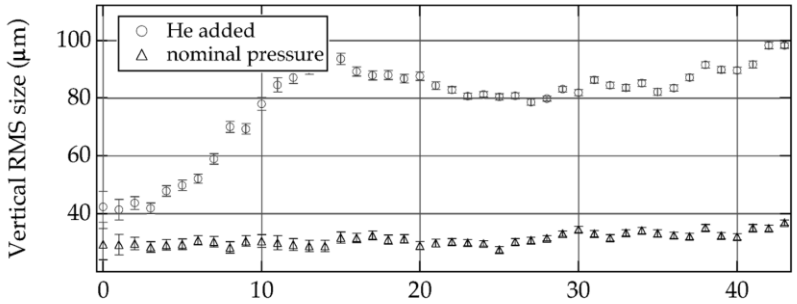

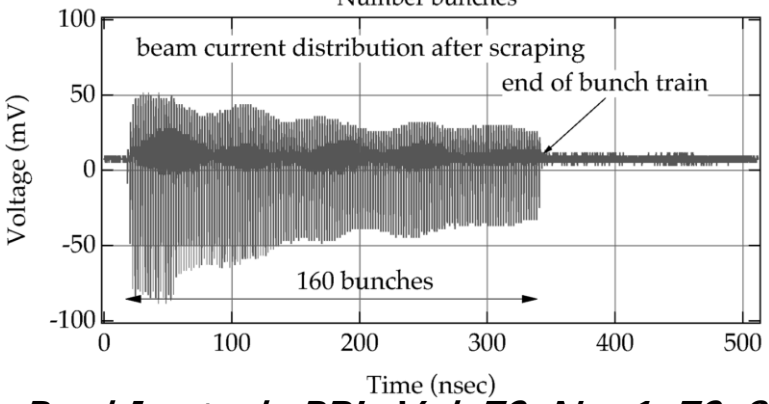

Byrd J., et. al., PRL, Vol. 79, No. 1, 79-82

◆ Bunch lengthening with harmonic cavity

- In the low- and medium-energy light sources, the beam lifetime reduce to several hours because of the Touschek scattering and low gaps of IDs. Harmonic cavities are used to increase beam lifetime in TOPUP injection by lengthening the bunch, and also provide tune spread to enhance Landau damping.

- Two RF systems: $V(\phi) = V_{RF}(\phi(t) + \phi_s) + V_h(n\phi(t) + n\phi_h)$

$$\frac{\sigma_z(V_{RF+harm})}{\sigma_z(V_{RF})} = \sqrt{\frac{\dot{V_{RF}}}{\dot{V_{RF+harm}}}} = \left(\frac{nV_{harm}}{V_{RF}}\cos(\phi_s) - 1\right)^{-\frac{1}{2}}$$

- The early applications of harmoni cavity were in Super-ACO and NSLS VUV-ring, followed by Elettra, SLS, and ALS etc. The cavity can be normal- and super- conducting, active and passive. Harmonic number varies from 3~5. The lengthening factors in the 3rd GLSs are about 3.

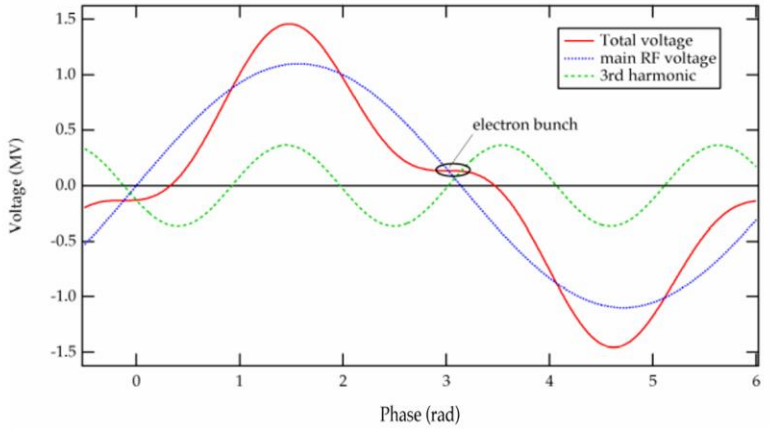

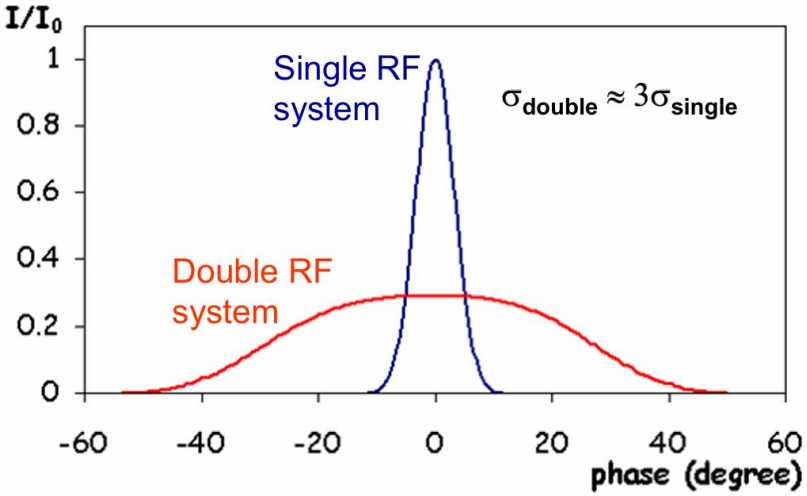

TOPUP Injection

◆ **Beam injection of the storage ring**

➢ **Beam injection with pulsed closed-orbit bump** is the most common method in the storage ring of the 3rd GLSs. SSRF as an example, the injection system consists of four kickers and two septums.

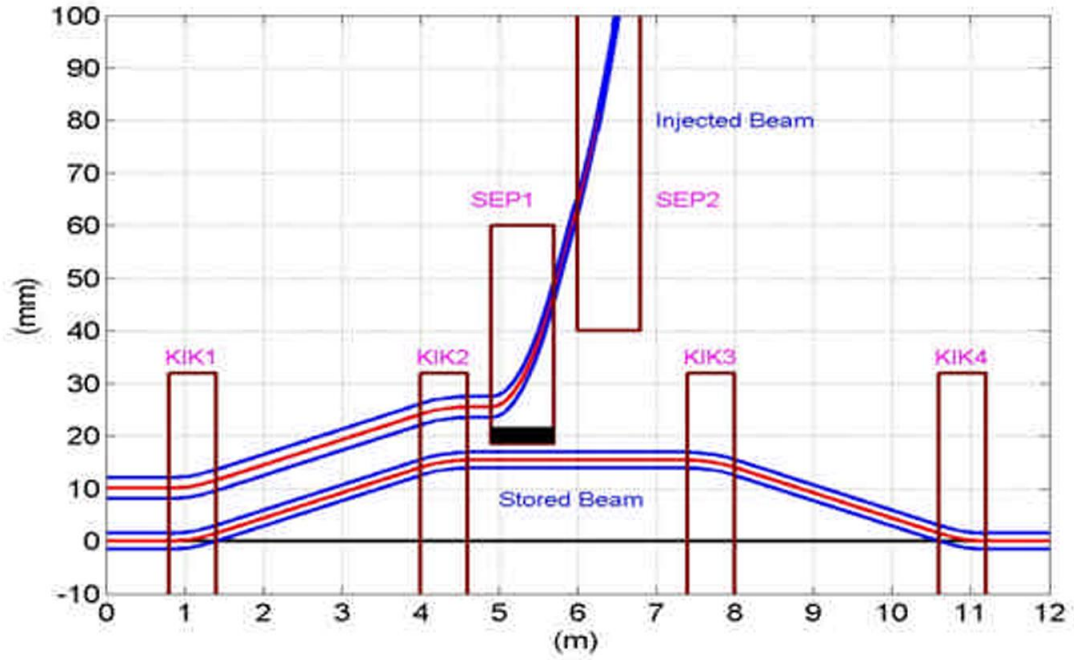

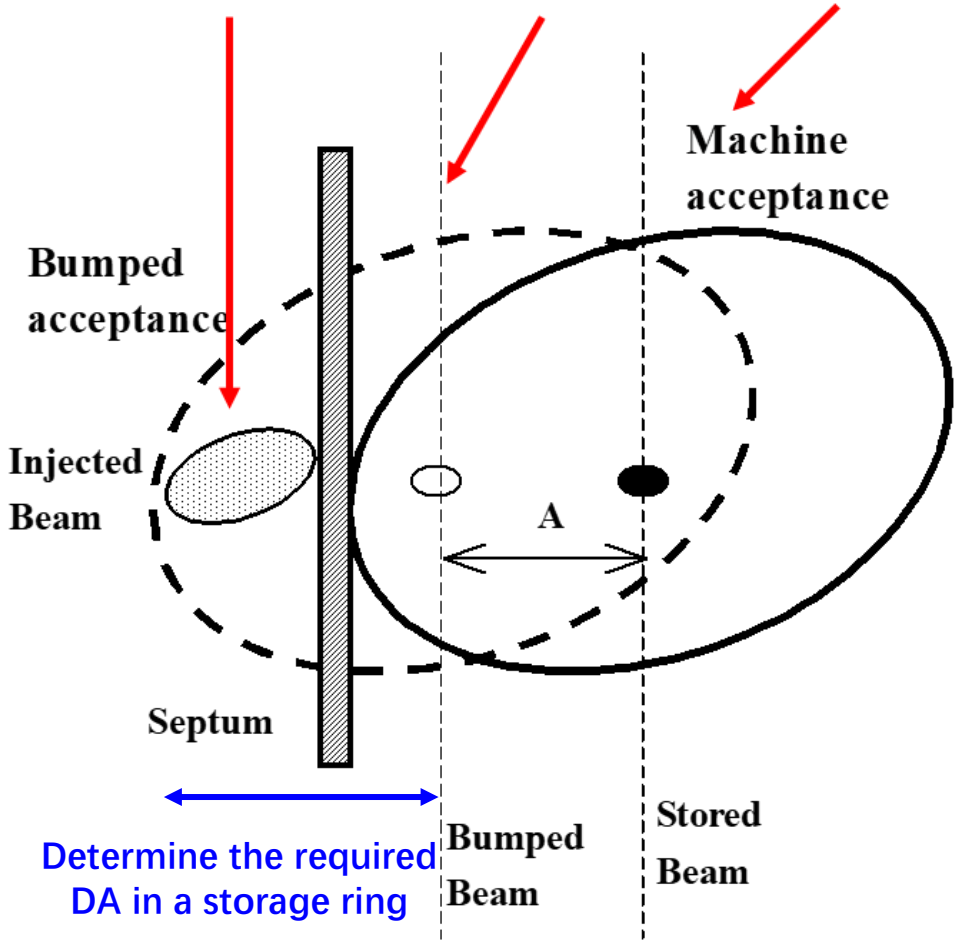

◆ TOPUP injection

- When the beam current drops to a certain value, immedetely compensate a fraction of currents. This method provides a constant beam current during users' experiments.

- The reason of TOPUP injection is strong focusing for low emittance and low-gap IDs make Toushek-scattering dominated lifetime reduced to ~10 hrs. Drop of the beam current causes the variation of heat loading in optical lens in beamlines and vacuume wall in the storage ring, leading **unstable photon path and electron orbit.**

- Adopted by most of all the 3rd and 4th generation light sources.

- TOPUP injection has a benefit of higher integral flux.

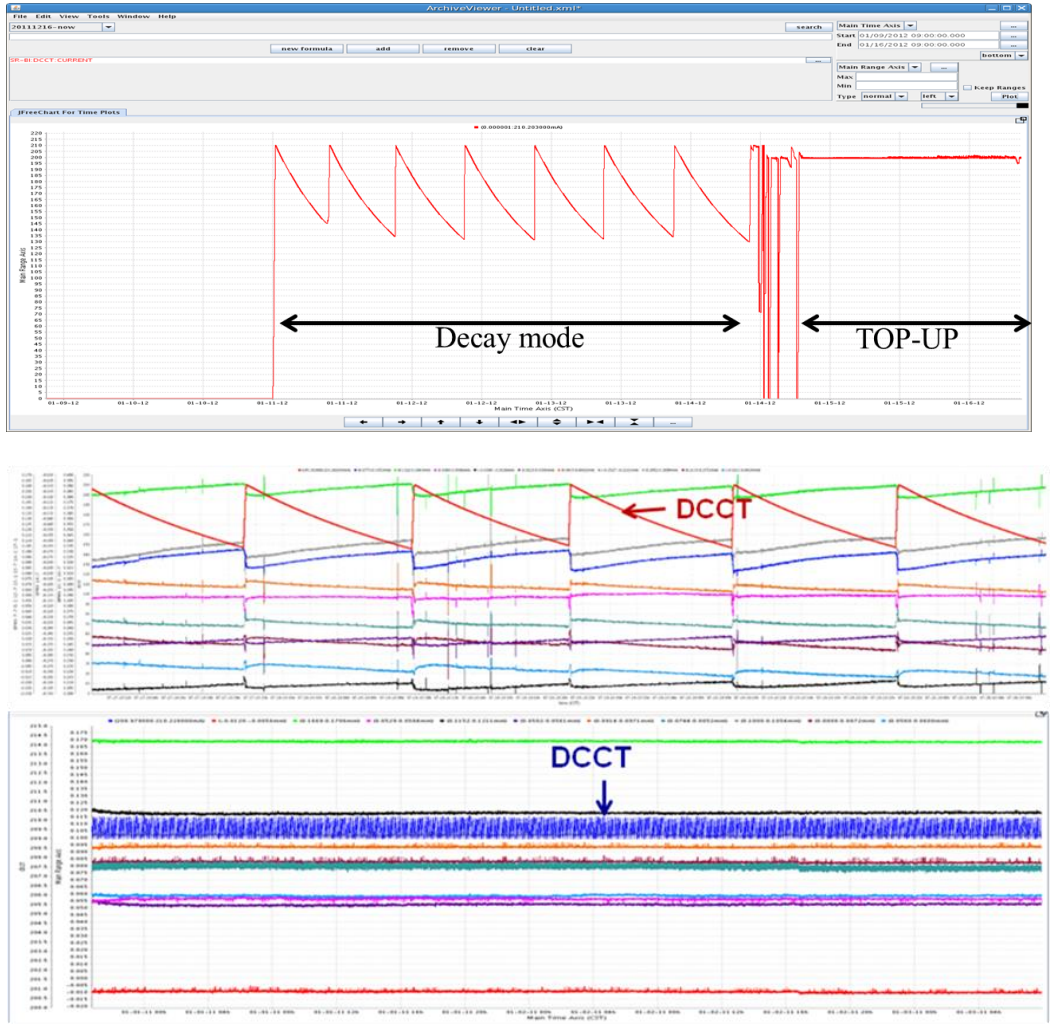

Stabilization of electron orbit by TOPUP injection in SSRF

- Key issue in TOPUP injection is **radiation safty** (because of opened optical shutters in the shield wall) that is ensured by the reliable interlock system. Any possibility of electron beam loss into beamline must be preclude.

- The interlock system should include real-time monitoring of beam status (especially the lifetime and the injection efficiency), hardware settings (power supplies), and radiation dose, etc.

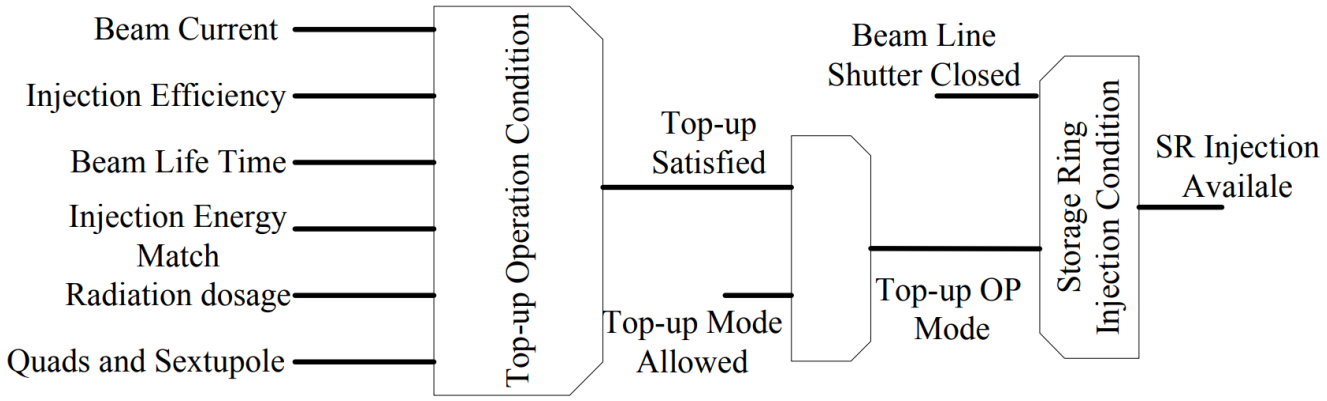

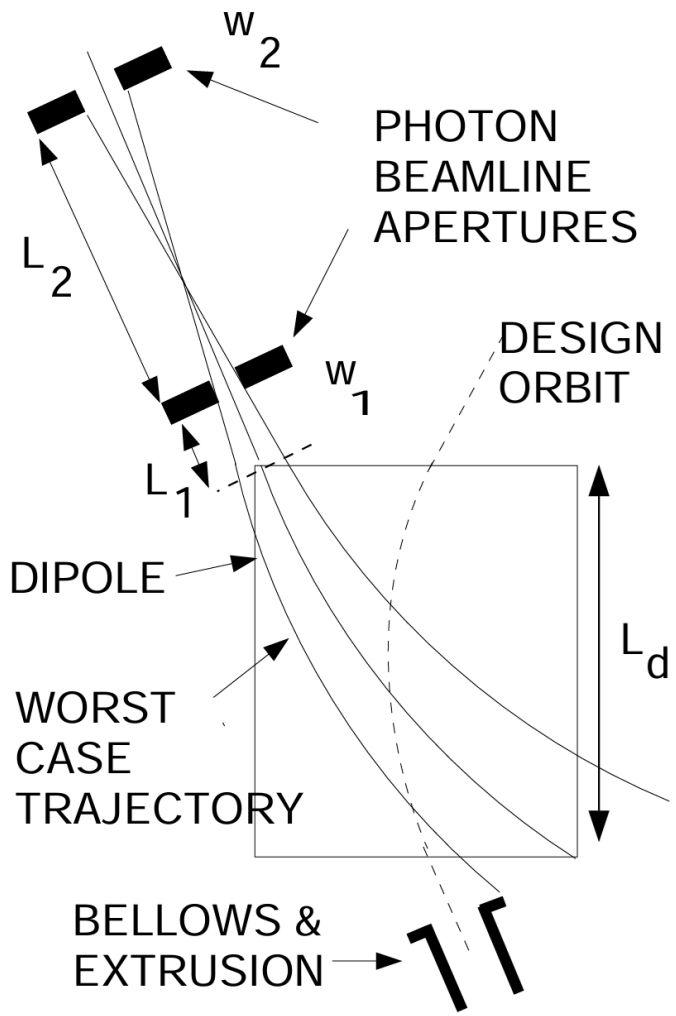

◆ Suppress of residual orbit disturbance

- A large injection disturbance will cause measured error in users' expriments.
- To suppress the residual orbit during TOPUP injection, SLS design the lattice with **long straight section** that can accommodate all the injection elements and avoid interaction between closed bump and multipoles.
- Many 3rd GLS facilities followed the design of long straight sections that impose **superperiod** in lattice.
- For more crucial expriments, gate signal of injection can help to delete the bad data.

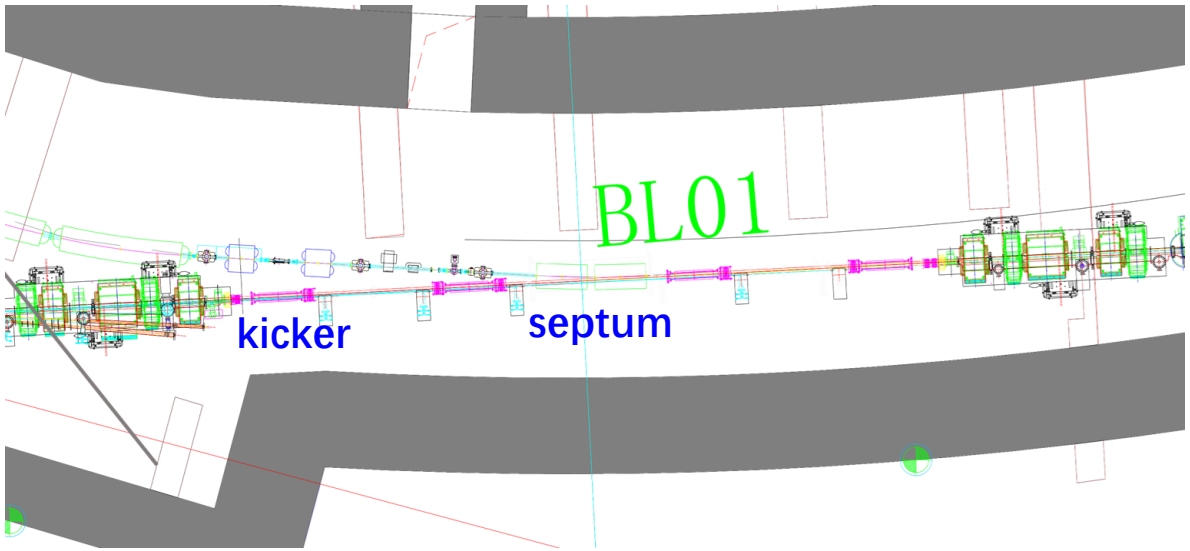

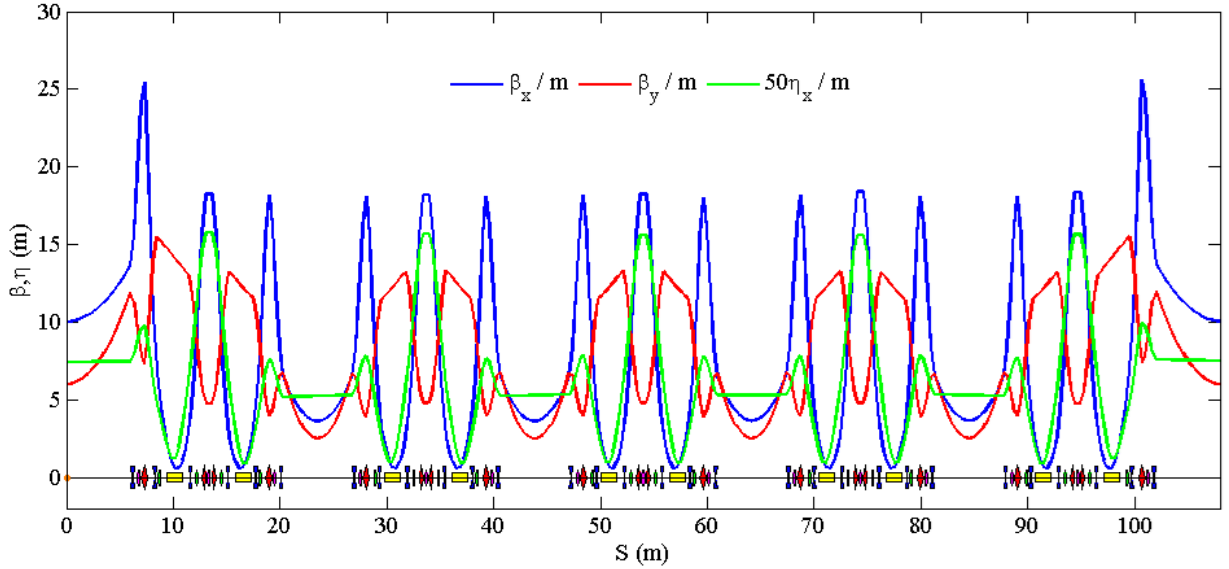

Outline

- The Way to the 3rd GLS
- Progress in the 3rd GLS
- **Overview of SSRF**
- Beam Dynamics in SSRF
- Summary

Overview of SSRF

◆ **Campus in Zhangheng Road** (Accommodating SSRF SXREL and a part of SHINE)

◆ SSRF Beamlines

➢ SSRF project (2004~2009): 7 beamlines **routine operation since May 2009** Fellow-up beam lines: 8

Disciplines	Beamlines	Source	Energy range	Scientific goals
Energy science	XAFS	Wigger	4.5~ 50keV	Energy conversion and storage
	SiP▪ME^2_NAP-XPS	BM	40eV-2keV	In situ electronic structure
	SiP▪ME^2_HR-ARPES	EPU	7-70eV	Electronic structures of novel quantum materials
Environ. Science	STXM	EPU	150-2000eV	Quantitative polymer and chemical mapping
	Hard X-ray Micro-focus	IVU	5keV-20keV	High pressure , environmental, biological science
Material Science	X-ray diffraction	BM	4-22 keV	Reveal crystal structure and property relationship
	Dreamline	EPU	20eV~2keV	Electronic structure of condensed matters
	X-ray imaging	SuperB	White beam Pink :8-40keV	Inner microstructure observation of materials
	SAXS	BM	5-20keV	Nanostructure characterization of materilals
Life Science	Macromolecular Crystallography	IVU	7-15keV	Determination of macromolecules & their complexes
	BioSAXS	IVU	7-15keV	Structure characterization for biomacromolecules&drugs
	High Throughput Crystallography	BM	5-20keV	High throughput protein crystallography
	Micro-Crystallography	IVU	5-18keV	Small crystal protein crystallography
	Complex Crystallography	IVU	7-15keV	Protein crystallography of large unit cell crystals
	FTIR and Microscope	BM	10-10000 cm^{-1}	Vibrational-rotational spectrum of biological molecules
Industry App	XIL	EPU	80-150eV	Nanostructures fabrication and EUV resist evaluation

- Phase-II project (2016-2024): 19 beam lines **34 beamlines and 46 experimental stations**
- Several extra users' beamlines are being in commissioning now.
  Full capacity ~40 beamlines as our earlier expection
- Apllication areas: Energy, environment, material, life science, and industrial applications

Disciplines	Beamlines	Source	Energy range	Scientific goals
Energy science	E-line	IVU+EPU	130eV~18keV	Energy conversion and control
	D-line	IVU+BM	10~ 10000cm^{-1} 5 ~ 25keV	Structure of non-equilibrium systems
	Radioactive materials	W	5~50keV	Radioactive material
	Hard X-Ray Spectroscopy	BM	5~30keV	Catalysis
Environ. Science	Hard X-ray Nanoprobe	IVU	5~25keV	Nano technology, cell, environ. components
	Medium-energy Spectroscopy	IVU	2.1~16keV	Environmental pollutants
	3D Nano Imaging	BM	5~14keV	Nano imaging
Material Science	S^2-resolved ARPES	Twin EPU	50~2000eV	Magnetic and electronic properties
	RIXS station	EPU	250~1700eV	Electronic structure
	Laue microdiffraction	Super B	7~30keV	Local microstructure and defects
	Surface diffraction	CPMU	4.8~28keV	Microstructure of surfaces and interfaces
	Laser Electron Gamma Source	ID	0.4~20MeV	Nuclear astrophysics/structure
Life Science	P2 Protein Crystallography	IVU	7~18keV	Moderate-risk infectious viruses
	Membrane Protein	IVU	7~15keV	Membrane protein
Industry Applications	Ultra Hard X-ray Applications	SCW	30~150keV	Engineering materials and rocks
	Time-resolved USAXS	IVU	8~15keV	Self-assembly and fiber-spinning
	Fast X-ray imaging	CPMU	8.7~30keV	Fast process imaging

SSRF Beamlines Map

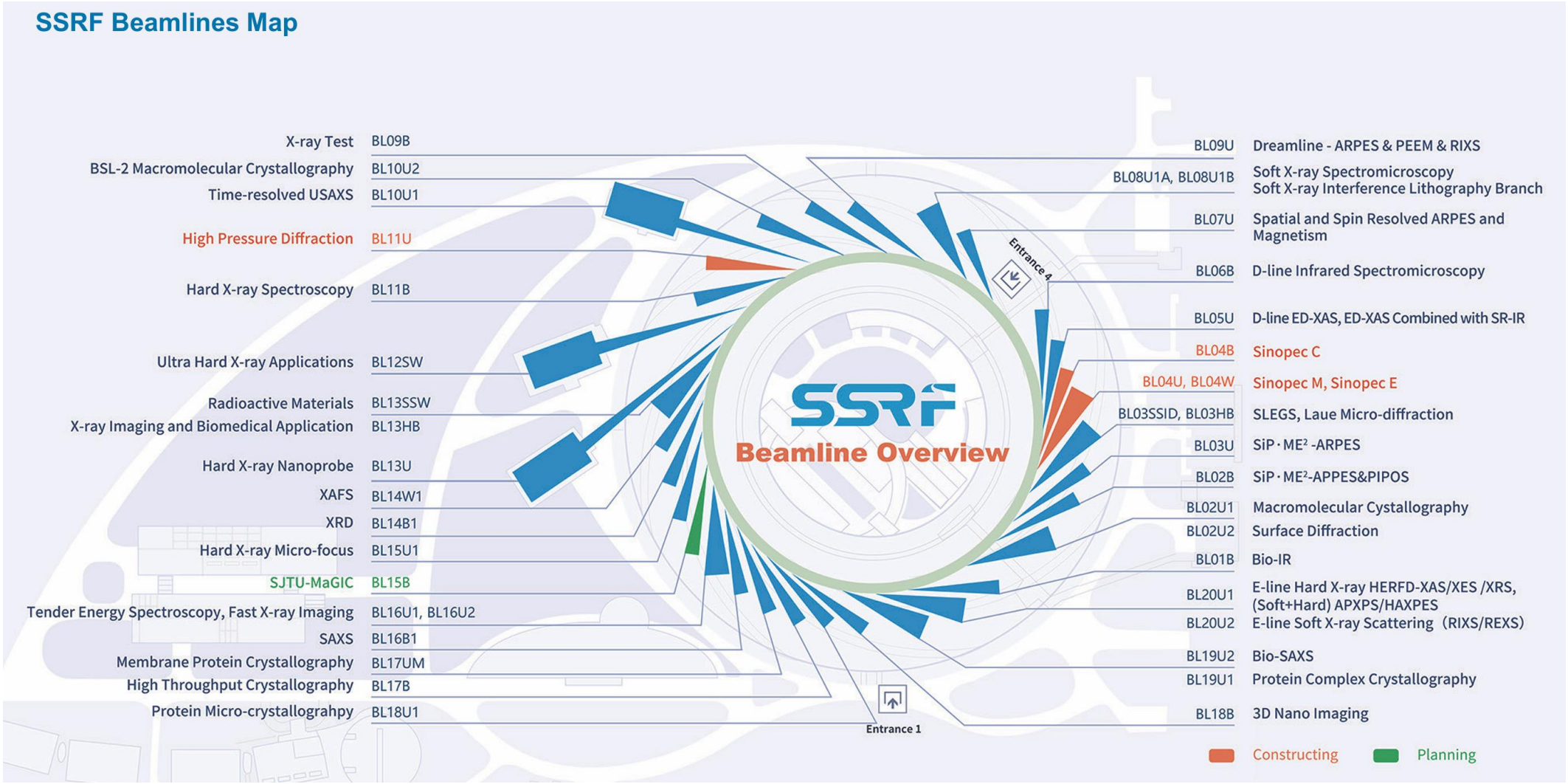

◆ Insertion Devices

- 25 IDs have been installed
- 6 different types
- 7 dual-canted IDs straights
- All of IDs were manufactured domesticaly

ID type	Number
IVU	12
CPMU	4
Wiggler	3
EPU	4 (+2)
AppleKnot EPU	1
SCW	1
Dual-Canted	5+2

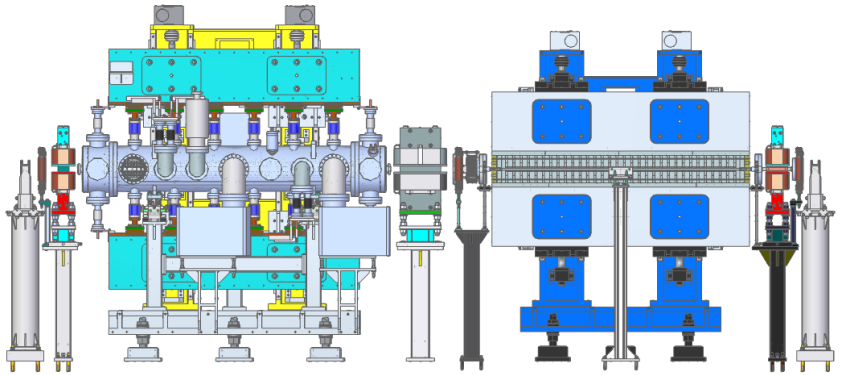

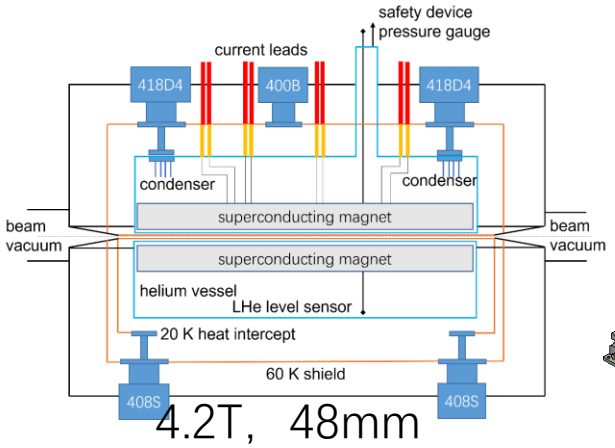

4.2T, 48mm

SCW

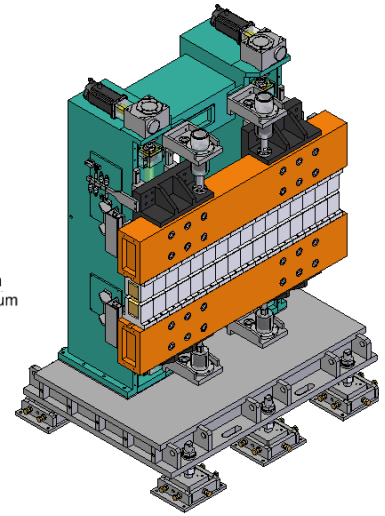

Wiggler

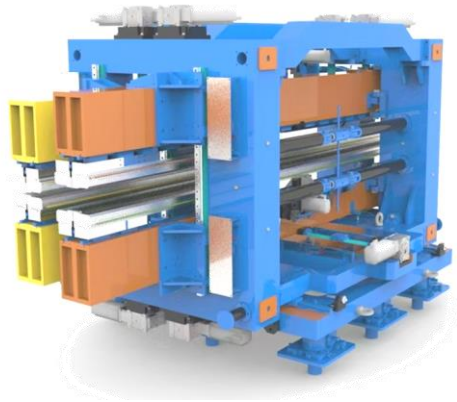

EPU

IVU

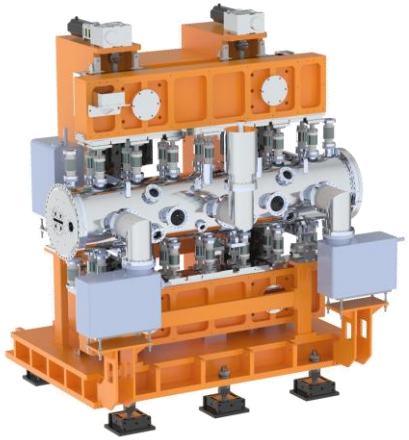

CPMU

Unit	Beamline	Photo Energy	ID	Periodicity	Gap	Field	Length
02	表面衍射线站	4.8-28 KeV	CPMU	20mm	6-30mm	1.09T	2.2m
02	生物大分子晶体学光束线站	7-15 KeV	IVU22N69	22mm	6-30mm	0.9T	2m
03	高分辨角分辨光电子能谱线站	7-70 eV	AppleKnotEPU200	200mm	16-80mm	0.7T	4.4m
05	动力学结构研究线站	5-25 KeV	IVU22	22mm	6-30mm	0.9T	2.6m
07	纳米自旋与磁学线站	50-2000 eV	Double EPU	58mm 90mm	16.5-150mm 18.8-150mm	0.78T 0.85T	5m
08	软X射线谱学显微光束线站	192 - 2182 eV	EPU100	100mm	35-98mm	0.6T	4.3m
09	“梦之线”	20-2000 eV	EPU58/148	58mm 148mm	16.5-120mm 22-130mm	0.78T 0.67T	5m
10	时间分辨超小角散射线站	8-15 KeV	IVU20	20mm	6-30mm	0.84T	2.1m
10	P2	7-18 KeV	IVU22	22mm	6-30mm	0.84T	2.1m
12	超硬多功能	30-150 KeV	SCW	48mm	9mm	4.2T	2.5m
13	稀有元素分析线站	5-50 KeV	Wiggle100	100mm	16.5-120mm	1.57T	1.5m
13	硬X射线纳米探针线站	5-25 KeV	IVU	20mm	6-30mm	0.86T	4.5m
14	XAFS光束线站	3.9 ~23 keV	wiggle80	80mm	14-140mm	1.3T	1.7m
15	硬X射线微聚焦及应用光束线站	5-20 keV	IVU25B	25mm	6-30mm	0.94T	2.7m
16	快X射线成像线站	8.7-30 KeV	CPMU	18mm	6-30mm	1.025T	3.6m
16	中能谱学线站	2.1-16 KeV	IVU	26mm	6-30mm	1.12T	3.6m
17	膜蛋白线站	5-25 KeV	CPMU	20mm	6-30mm	1.09T	3.7m
18	蛋白质微晶体结构光束线站	5-18 keV	IVU25C	25mm	6-30mm	0.96T	2.7m
19	蛋白质复合物晶体结构线站	7-15 keV	IVU20A	20mm	7-30mm	1.04T	2.2m
19	生物小角散射线站	7-15 keV	IVU20A	20mm	7-30mm	1.04T	2.2m
20	能源材料线站	130 eV-18 KeV	IVU24	24mm	6-30mm	0.96T	2.1m
			EPU60	60mm	14.5-85mm	0.90T	1.9m

◆ Photon spectra

- Avaibable photon spectrum in SSRF ranges from Infrared (Dipole eddy) to ultra hard X ray (SCW) and Gamma Ray (SLEGS).
- Most of all the beamlines use X-ray (3~30keV), which have optimal high flux and brightness in medium-energy light sources.

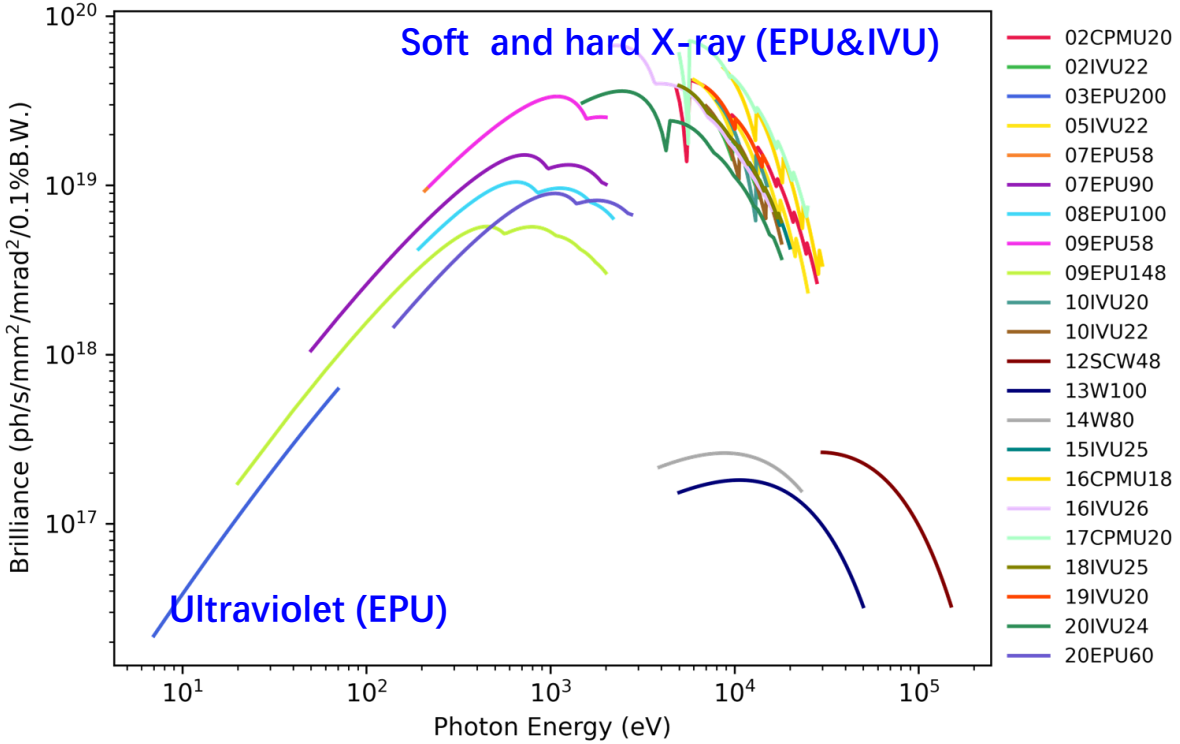

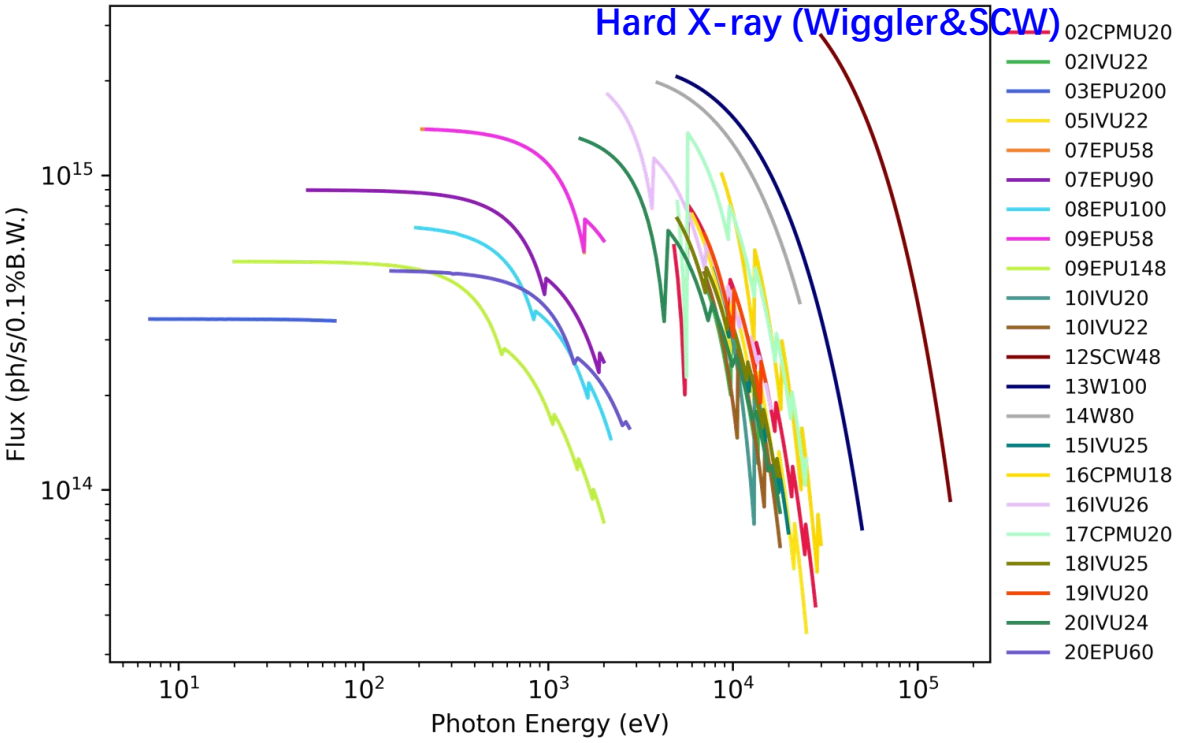

◆ SSRF Accelerator Complex

- LINAC + Booster + Storage ring
- 2×Transport lines

LINAC		
Beam energy	MeV	158
Charge (Single/Multi)	nC	1.0/3.0
Normalized emittance	mm.mrad	50
Energy spread		0.5%
BOOSTER		
Circumference	m	180
Beam energy	GeV	0.158→3.5
Extracted beam emittance	nm.rad	100
Repetition rate	Hz	2
STORAGE RING		
Circumference	**m**	**~432**
Structure		**20×DBA**
Beam energy	**GeV**	**3.5**
Beam current	**mA**	**200~300**

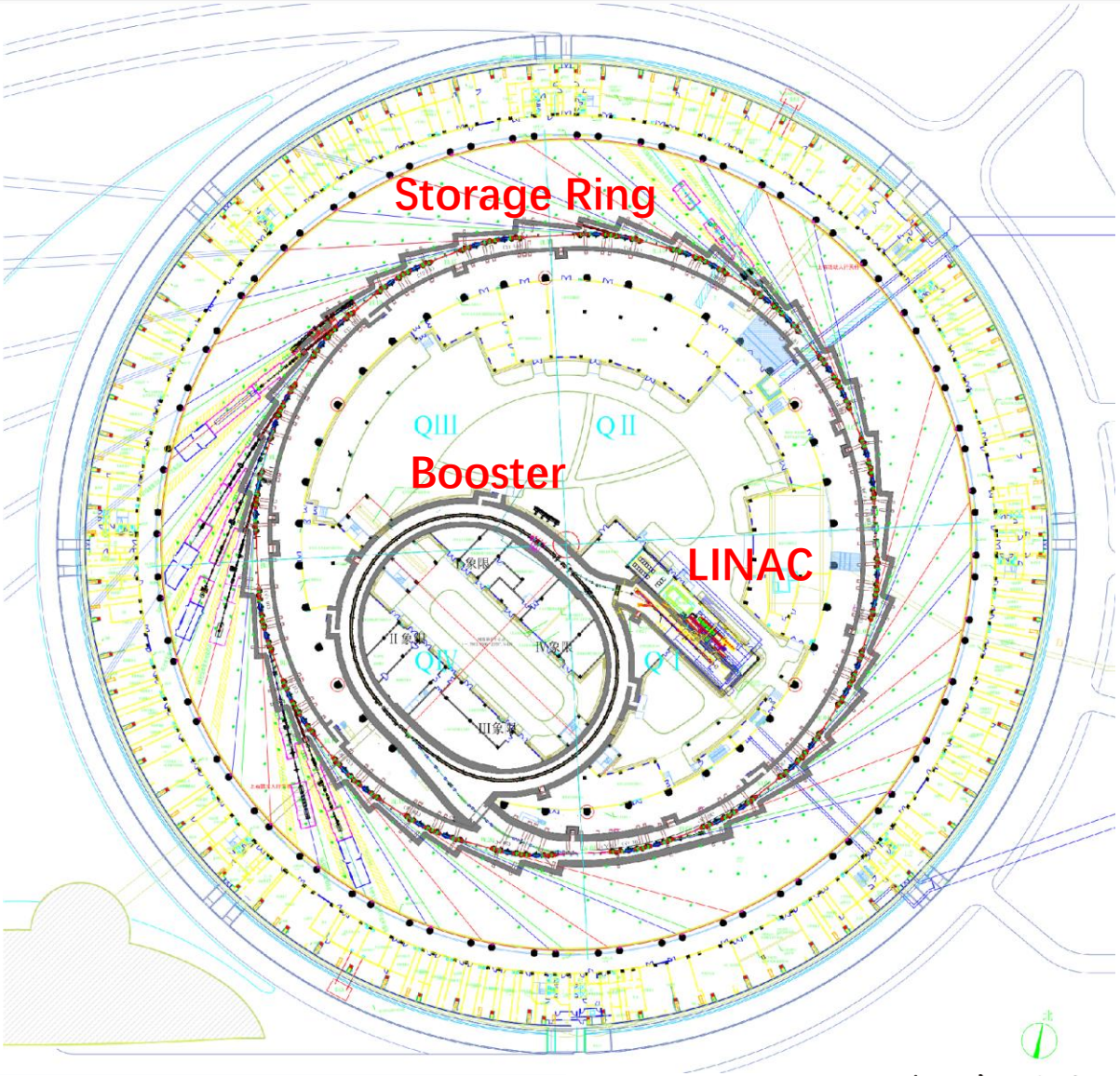

Operation Status

- **Web of the SSRF operation**
  - https://status.ssrf.ac.cn/ssrf/beam/beian.miit.gov.cn
  - Real-time measured beam parameters and brief status of all the beamlines

SSRF Operation Status

Main parameters

Current: 200.17mA

Energy:	3.5GeV
Emittance:	4.8nm-rad
Beam life time:	15.63hours
IntgCurrent:	20210.47AH
AveragePre:	3.29e-10Torr
Tune(x/y):	22.230/12.167
Hor.beamsize:	75.5um
Ver.beamsize:	69.7um
Coupling:	0.60%
Orbit(rms)x/y:	69.67/79.21um

operator: **shift plan:User Time light: Available**

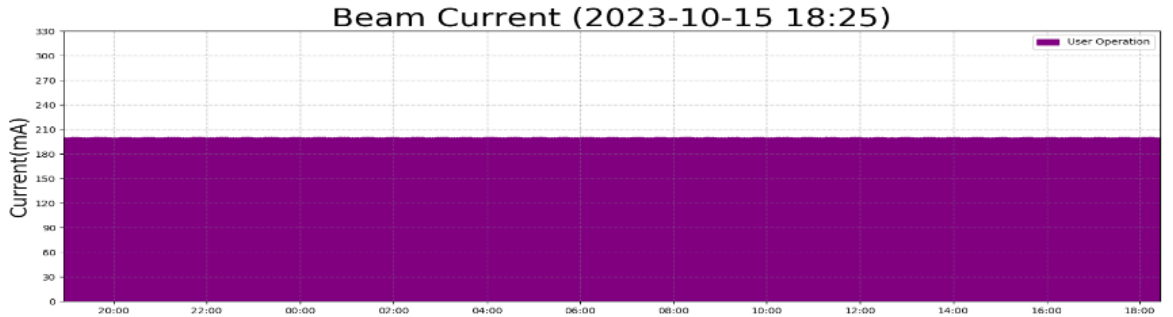

Beam Image

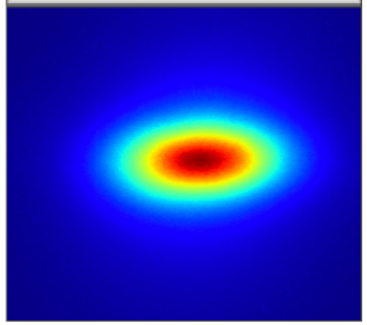

Beamline status

Beamline	ID status	Shutter status	Beamline	ID status	Shutter Status	Beamline	ID status	Shutter Status
BL01B1	--	Open	BL08U1B	71.953mm	Open	BL14B	--	Open
BL02B1		Open	BL09U58	160.002mm	Open	BL15U1	6.741mm	Open
BL02U1	7.380mm	Open	BL09U148	59.181mm	Open	BL16B1	--	Open
BL02CPMU	5.999mm	Open	BL09B1		Open	BL16U1	10.401mm	Closed
BL03HB	--	Open	BL10U1	7.299mm	Open	BL16U2	8.000mm	Open
BL03U1	65.745mm	Open	BL10U2	7.533mm	Open	BL17B	--	Open
BL03SS	--	Open	BL11B1		Open	BL18U1	7.167mm	Open
BL05U1	5.998mm	Open	BL12SCW		Closed	BL19U1	9.368mm	Open
BL06B1		Open	BL13HB		Open	BL19U2	8.597mm	Open
BL07U58	25.117mm	Open	BL13IVU	7.151mm	Open	BL20U1	7.499mm	Open
BL07U90	150.000mm	Open	BL13SSW	16.500mm	Closed	BL20U2	28.900mm	Open
BL08U1A	71.953mm	Open	BL14W	17.000mm	Open			

Message from control room:


中国科学院
CHINESE ACADEMY OF SCIENCES
Light & Truth
2024-05-15 星期三 17:12:58
SRF
DELL

◆ Machine Time

- ~7000 hrs operation
- ~4500 hrs for users' experiments
- ~2500 hrs for warmup, machine studies and in-house study.

SSRF Operation Schedule (Jan1-Dec 31, 2025)

Jan			Feb			Mar			Apr			May			June			July			Aug			Sep			Oct			Nov			Dec		
1	B	B	1	D	D	1	B	B	1	M	A	1	U	U	1	U	U	1	M	A	1	D	D	1	A	A	1	B	B	1	U	U	1	U	U
2	U	U	2	D	D	2	B	B	2	B	B	2	U	U	2	U	U	2	A	A	2	D	D	2	A	A	2	U	U	2	U	U	2	M	A
3	U	U	3	D	D	3	U	U	3	U	U	3	U	U	3	M	A	3	B	B	3	D	D	3	B	B	3	U	U	3	U	U	3	B	B
4	U	U	4	D	D	4	U	U	4	U	U	4	U	U	4	A	A	4	U	U	4	D	D	4	B	B	4	U	U	4	M	A	4	U	U
5	U	U	5	D	D	5	U	U	5	U	U	5	U	U	5	B	B	5	U	U	5	D	D	5	U	U	5	U	U	5	A	A	5	U	U
6	U	U	6	D	D	6	U	U	6	U	U	6	M	A	6	U	U	6	U	U	6	D	D	6	U	U	6	U	U	6	B	B	6	U	U
7	M	A	7	D	D	7	U	U	7	U	U	7	A	A	7	U	U	7	U	U	7	D	D	7	U	U	7	U	U	7	U	U	7	U	U
8	A	A	8	D	D	8	U	U	8	M	A	8	B	B	8	U	U	8	M	A	8	D	D	8	U	U	8	M	A	8	U	U	8	U	U
9	B	B	9	D	D	9	U	U	9	A	A	9	U	U	9	U	U	9	B	B	9	D	D	9	M	A	9	B	B	9	U	U	9	M	A
10	U	U	10	D	D	10	U	U	10	B	B	10	U	U	10	M	A	10	U	U	10	D	D	10	B	B	10	U	U	10	U	U	10	B	B
11	U	U	11	D	D	11	M	A	11	U	U	11	U	U	11	B	B	11	U	U	11	D	D	11	U	U	11	U	U	11	M	A	11	U	U
12	U	U	12	D	D	12	B	B	12	U	U	12	U	U	12	U	U	12	U	U	12	D	D	12	U	U	12	U	U	12	B	B	12	U	U
13	U	U	13	D	D	13	U	U	13	U	U	13	M	A	13	U	U	13	U	U	13	D	D	13	U	U	13	U	U	13	U	U	13	U	U
14	M	A	14	D	D	14	U	U	14	U	U	14	B	B	14	U	U	14	U	U	14	D	D	14	U	U	14	M	A	14	U	U	14	U	U
15	B	B	15	D	D	15	U	U	15	M	A	15	U	U	15	U	U	15	D	D	15	D	D	15	U	U	15	A	A	15	U	U	15	U	U
16	U	U	16	D	D	16	U	U	16	B	B	16	U	U	16	U	U	16	D	D	16	D	D	16	M	A	16	B	B	16	U	U	16	M	A
17	U	U	17	W	W	17	U	U	17	U	U	17	U	U	17	M	A	17	D	D	17	D	D	17	A	A	17	U	U	17	U	U	17	A	A
18	U	U	18	W	W	18	M	A	18	U	U	18	U	U	18	A	A	18	D	D	18	D	D	18	B	B	18	U	U	18	M	A	18	B	B
19	U	U	19	W	W	19	A	A	19	U	U	19	U	U	19	B	B	19	D	D	19	D	D	19	U	U	19	U	U	19	A	A	19	U	U
20	U	U	20	W	W	20	B	B	20	U	U	20	M	A	20	U	U	20	D	D	20	D	D	20	U	U	20	U	U	20	B	B	20	U	U
21	D	D	21	W	W	21	U	U	21	U	U	21	A	A	21	U	U	21	D	D	21	D	D	21	U	U	21	M	A	21	U	U	21	U	U
22	D	D	22	A	A	22	U	U	22	M	A	22	B	B	22	U	U	22	D	D	22	W	W	22	U	U	22	B	B	22	U	U	22	U	U
23	D	D	23	A	A	23	U	U	23	A	A	23	U	U	23	U	U	23	D	D	23	W	W	23	M	A	23	U	U	23	U	U	23	M	A
24	D	D	24	A	A	24	U	U	24	B	B	24	U	U	24	M	A	24	D	D	24	W	W	24	B	B	24	U	U	24	U	U	24	B	B
25	D	D	25	A	A	25	M	A	25	U	U	25	U	U	25	B	B	25	D	D	25	W	W	25	U	U	25	U	U	25	M	A	25	U	U
26	D	D	26	A	A	26	B	B	26	U	U	26	U	U	26	U	U	26	D	D	26	W	W	26	U	U	26	U	U	26	B	B	26	U	U
27	D	D	27	A	A	27	U	U	27	U	U	27	M	A	27	U	U	27	D	D	27	A	A	27	U	U	27	U	U	27	U	U	27	U	U
28	D	D	28	A	A	28	U	U	28	U	U	28	B	B	28	U	U	28	D	D	28	A	A	28	U	U	28	M	A	28	U	U	28	U	U
29	D	D				29	U	U	29	M	A	29	U	U	29	U	U	29	D	D	29	A	A	29	U	U	29	A	A	29	U	U	29	U	U
30	D	D				30	U	U	30	B	B	30	U	U	30	U	U	30	D	D	30	A	A	30	M	A	30	B	B	30	U	U	30	M	A
31	D	D				31	U	U				31	U	U				31	D	D	31	A	A				31	U	U				31	B	B
Jan			Feb			Mar			Apr			May			June			July			Aug			Sep			Oct			Nov			Dec		

U	User Time	B	Beamline Study
A	Machine Study	D	Shutdown, Installation
M	Maintenance	W	Warm Up

◆ Availability for Users' Experiments

- Increased in the first several years, while be significantly affected by the following projects.
- It is desired that the availability could increase from now on, since the Phase-II project has been successfully completed.

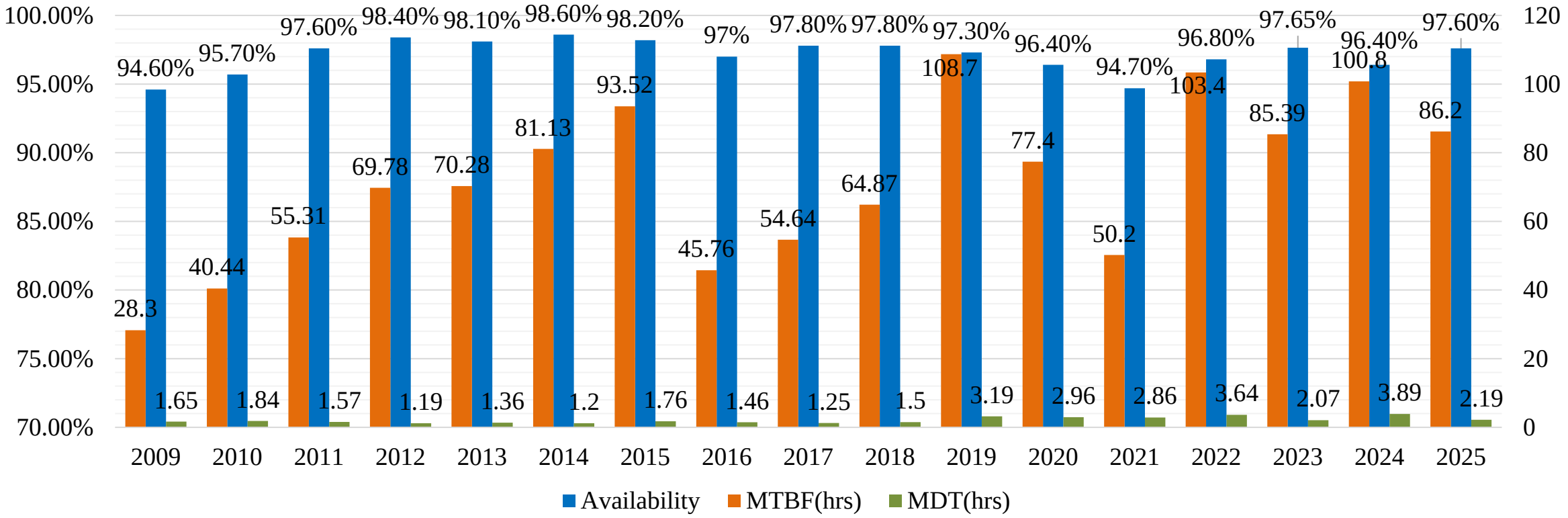

◆ Hardware Failures

- Observable hardware failures directly shown in the control panel.
- Hardware failures without direct indication/tangible evidence can be easily identified with beam behaviors.

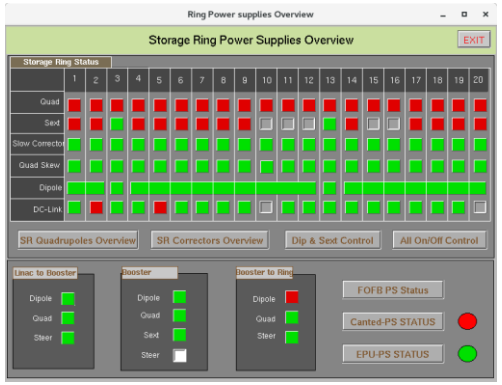

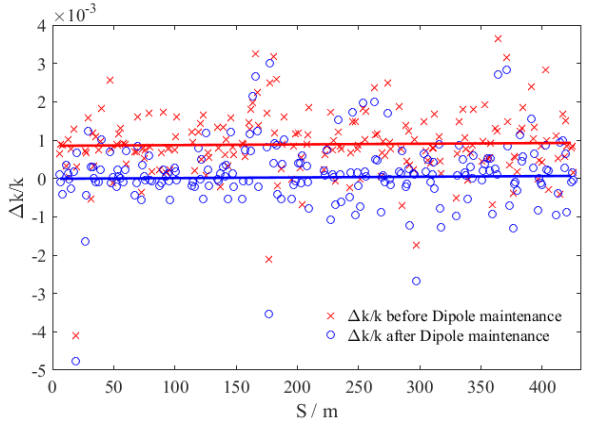

- While RF system (Arc of Coupler) and SCW (Quench) imposed significant challenge to the reliability. (Replace with spare equipments)

Time proportion	2024	2023	2022	2021	2020
RF	16.41%	5.16%	6.93%	3.95%	13.1%
Power Supply	7.16%	29.6%	22.9%	10.5%	19.9%
Cryogenic System	2.95%	0	24.6%	17.9%	7.74%
SCW	38.7%	17.0%	----	----	----
Utility	9.61%	19.9%	5.12%	6.27%	9.44%
Front End	5.32%	7.65%	12.2%	22.3%	7.33%
Diagnosis	4.27%	0	9.71%	10.9%	3.35%
Control System	2.40%	1.43%	0.27%	0.16%	3.20%
Electronic System	0.20%	0	0	5.14%	0
Pulsed Equipment	3.81%	5.38%	0	9.51%	0.77%
Vacuum	0	0.12%	9.11%	1.66%	0
Acce. Technology	2.83%	8.87%	8.83%	0.17%	0.99%
Radiation Prot.	1.18%	1.03%	0.35%	0	0.38%
Operation	0	2.38%	0	0	0
Others	5.10%	1.49%	0	11.5%	33.9%

Outline

- The Way to the 3rd GLS
- Progress in the 3rd GLS
- Overview of SSRF
- **Beam Dynamics in SSRF**
- Summary

Lattice Design of the Storage Ring

◆ Lattice Structure and beam dynamics

- Chasman-Green lattice (Double-Bend-Achromat): simplest focusing structure for optimizing source points and global properties of the storage ring.

- 20 DBA cells and 16 stardrd straight sections and 4 long straight sections.

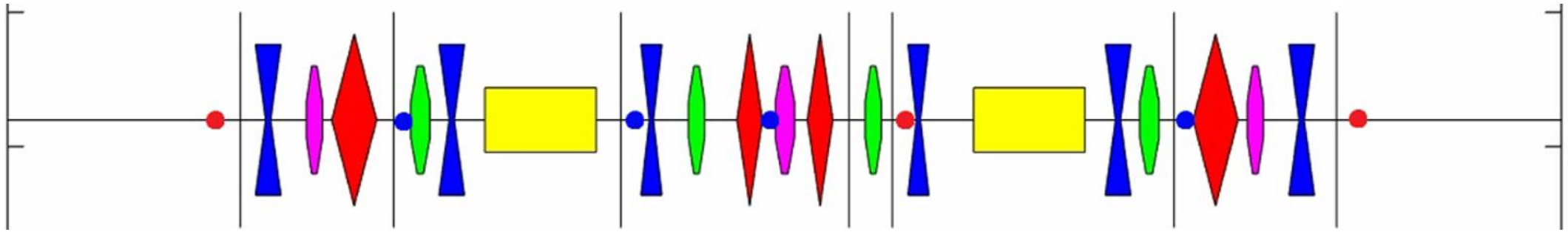

Each cells in SSRF-Ring consists of 2 dipoles, 10 quadrupoles, 7 sextupoles, 4 soft correctors, 3 fast correctors, 7 BPMs, and 4 skew quadrupole coils.

- TME in the SSRF storage ring

$$\varepsilon_{x,TME,Achro.} = 4.5nm.rad \qquad \varepsilon_{x,TME,Chro.} = 1.5nm.rad$$

- For a reasonable gradients, acceptable beam envelope, and well separation between β functions, the natural emittance in the SSRF storage ring was optimized down to 3.9 nm.rad, two and half times of the TME.

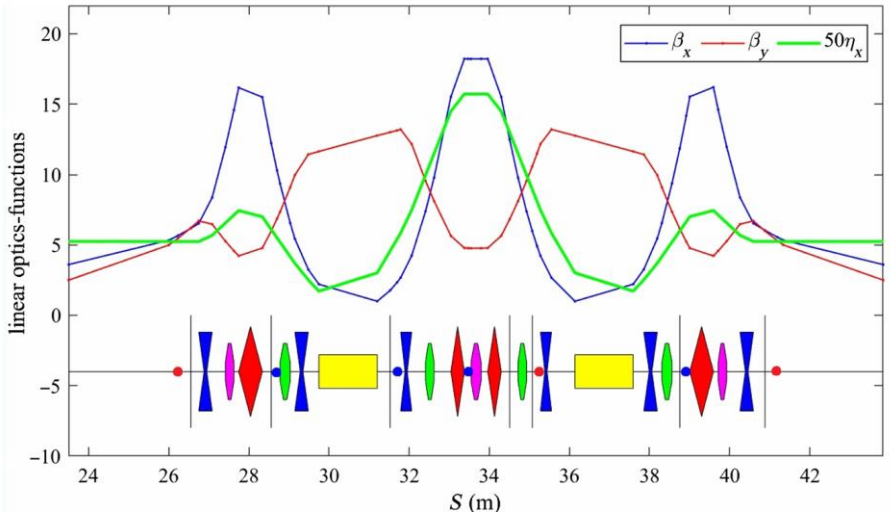

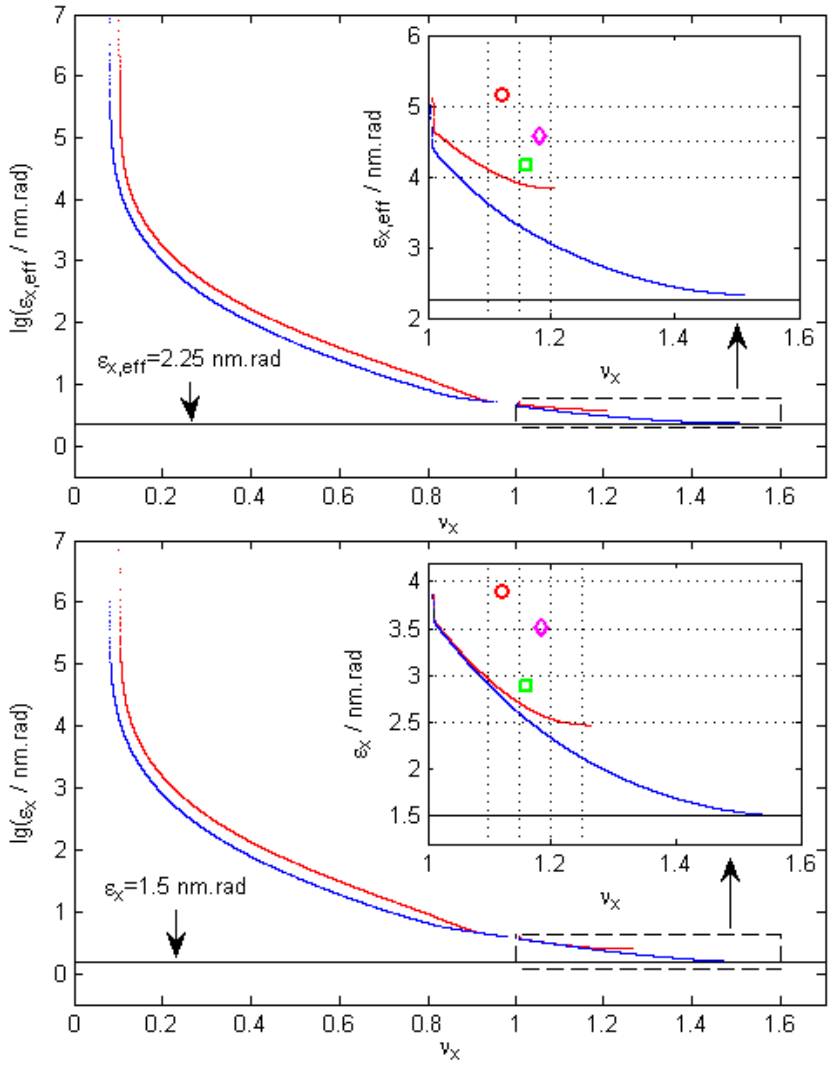

- Original lattice: Ideal four-fold symmetry/periodicity. Had been routinely operated for ten years (2009~2018)

- Phase-II project required necessary modification.

- More space for the planned IDs ← modification of arc section
- Higher flux of hard X-ray from dipole ← Super-Bend
- Dual-Canted ID in long SS ← double mini/waist beta-y optics
- Superconducting wiggler ← eliminate dispersion in its SS

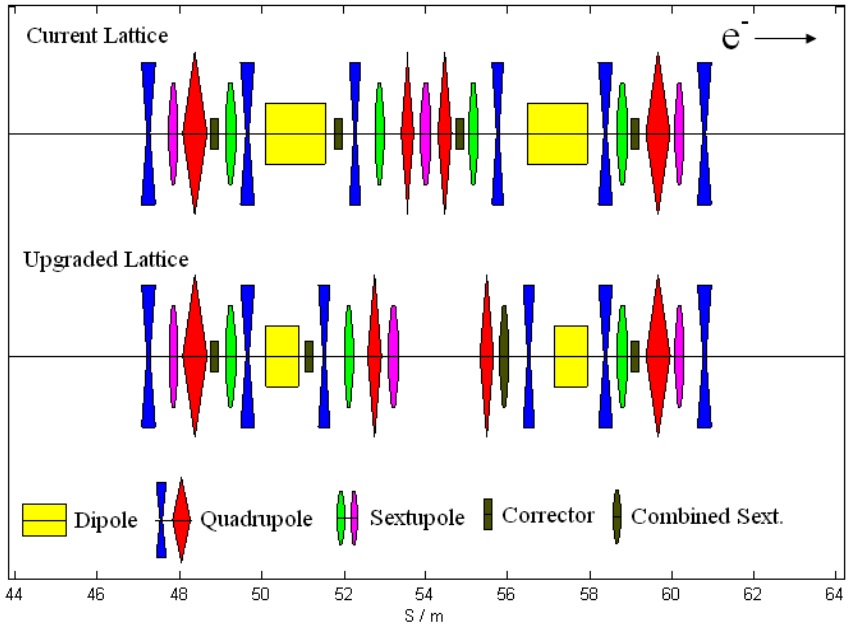

Blueprints of SCW (peak field ~4.2 T) and SuperB (2.29 T)

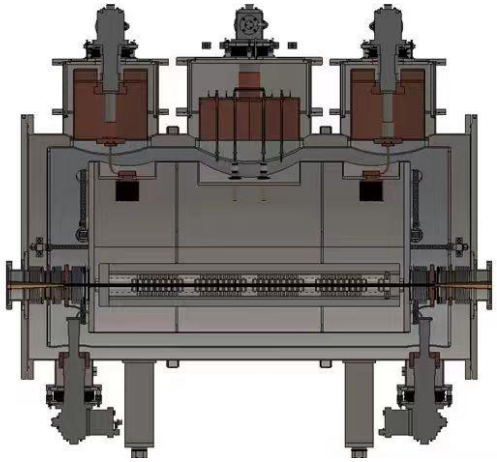

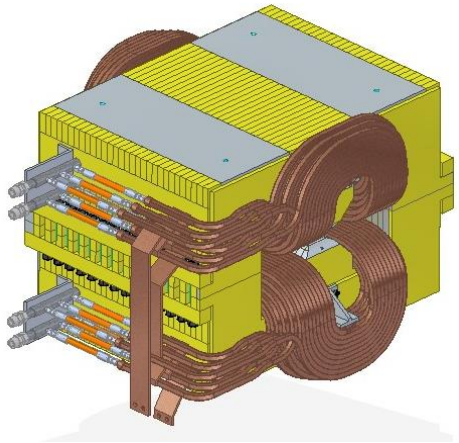

Modification in one DBA cell
Sketch of double waist design in LSS

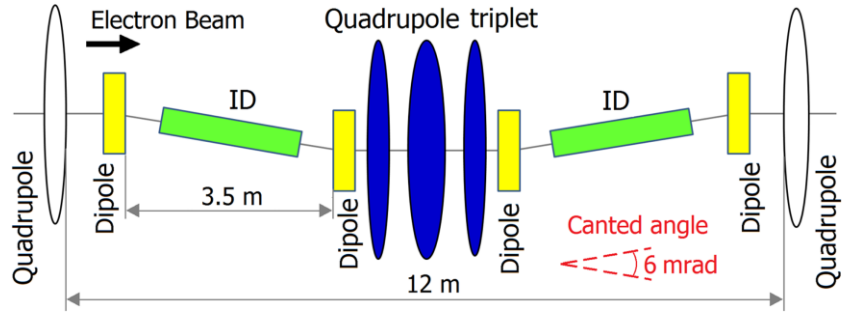

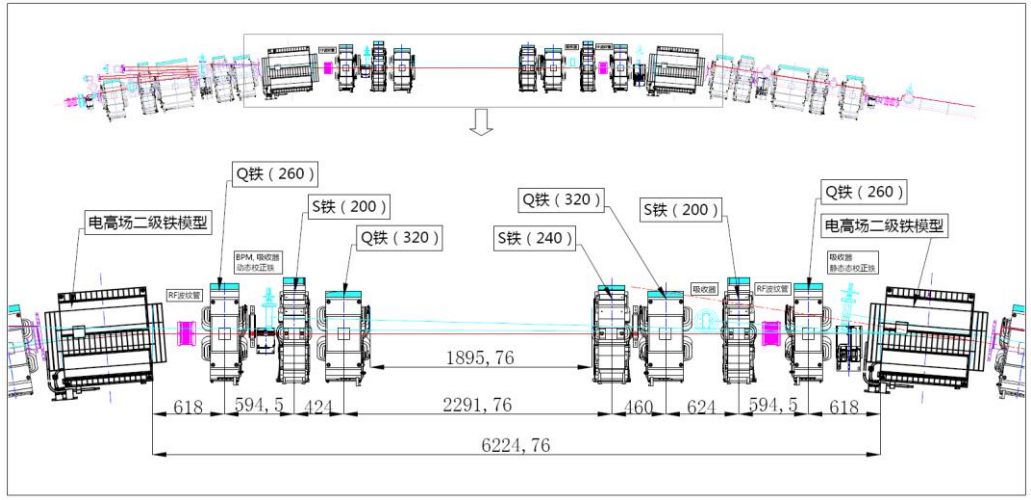

Layout of the arc section in SuperB cell

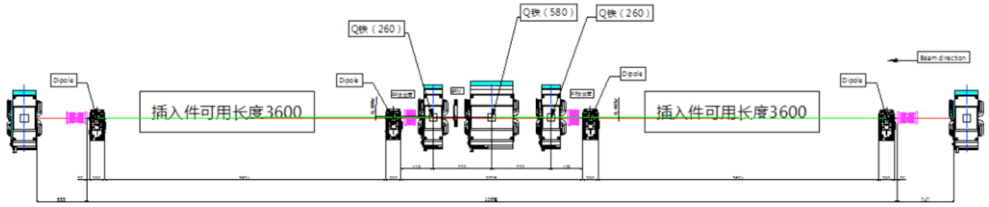

Layout of the long straight section

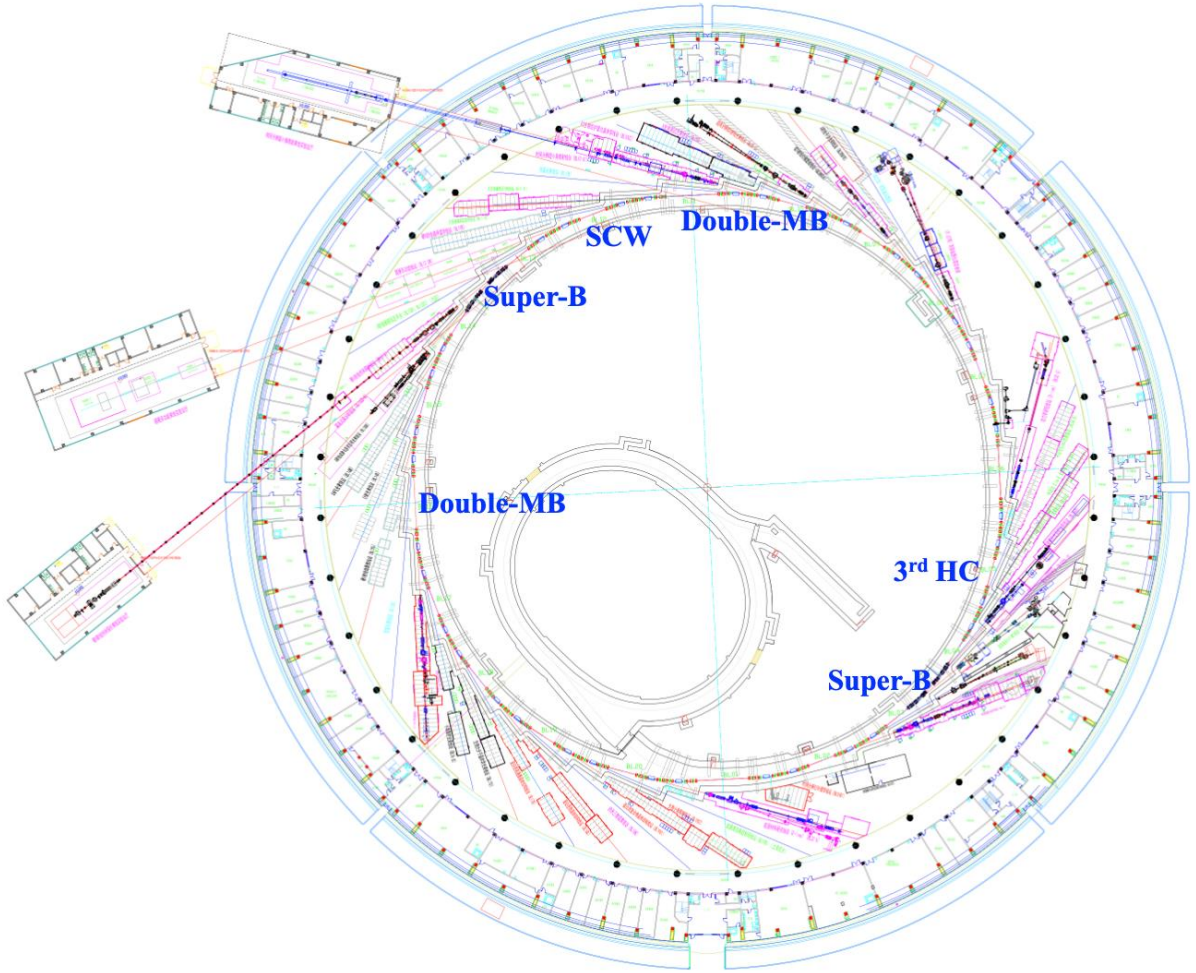

A quarter of the ring has been upgraded, and the original symmetry or periodicity has been destroyed.

- Design/optimization strategy consisted of:

① The same phase advance in SuperB cell as the nominal cell
② Pi-trick in double waist section
③ More sextupole families were classified according to beam optics (8→16)
④ Global fine-tuning with GA

- A new lattice with 4.2 nm.rad of beam emittance, and sufficient DA and EA for beam injection and lifetime.

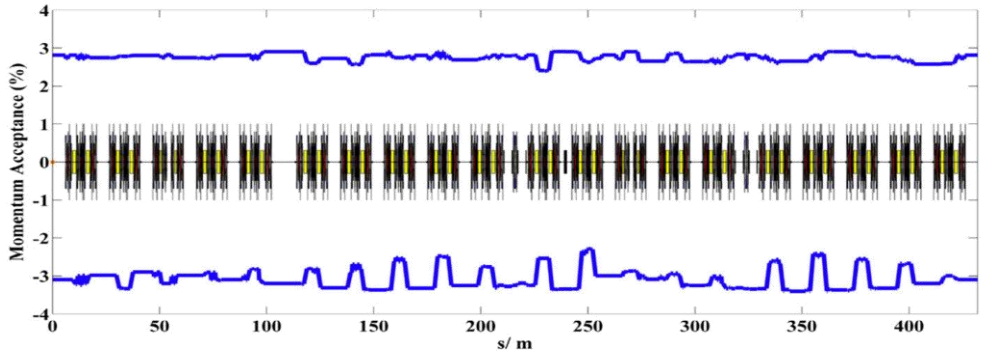

Fig. 8. Global momentum acceptance of the new SSRF storage ring lattice.

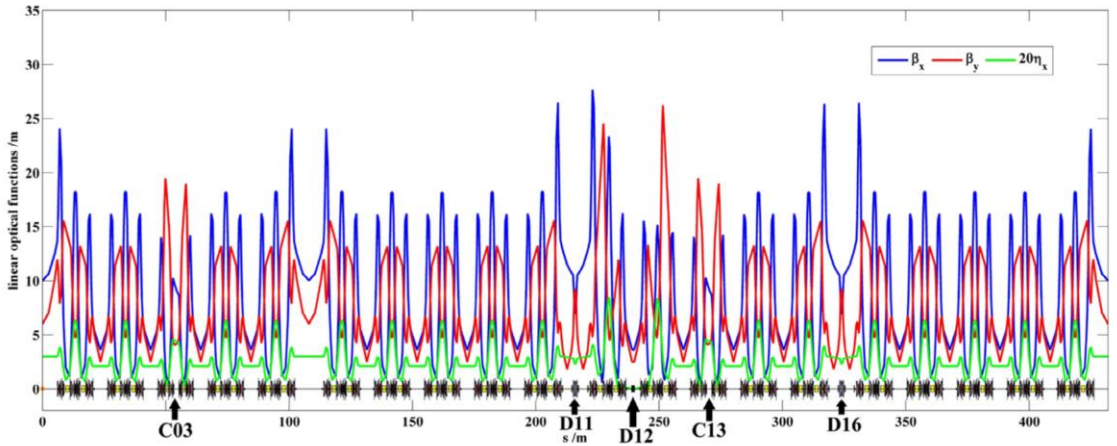

Fig. 2. Linear optics of the new SSRF storage ring lattice.

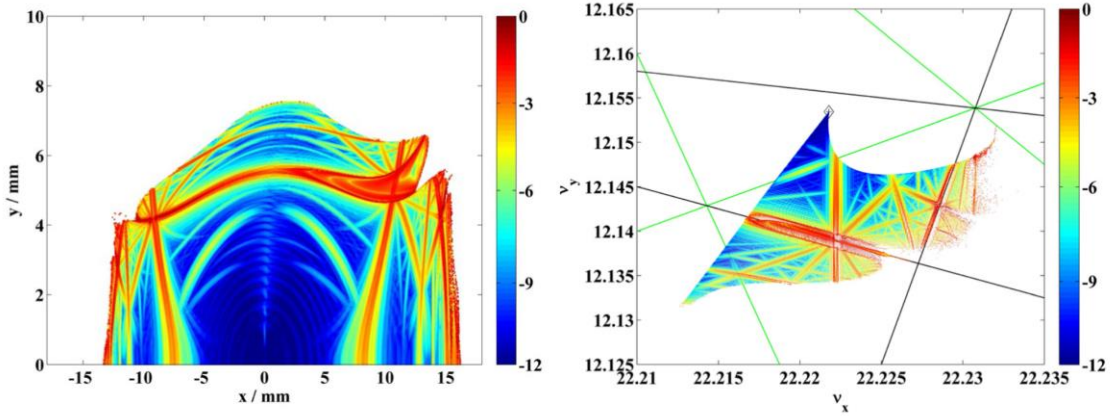

Fig. 7. Diffusion map (left) and frequency map (right) of the on-momentum dynamic aperture.

◆ Beam Parameters of the Storage Ring

Parameter	Original	Upgraded	Measured
Beam energy / GeV	3.5	3.5	3.50±0.01
Circumference / m	432	431.9893	431.965±0.003
Beam current / mA	200~300	200~300	200~260
Beam lifetime / hrs	>15 (200mA)	~12 (200mA)	18.0±0.5 (200mA, HC)
Working point (H, V)	22.22, 11.29	22.222, 12.153	22.222/12.153 (±0.002)
Natural chromaticity (H, V)	-55.7, -18.0	-55.3, -20.4	-51/-19 (±5/±3)
Natural emittance / nm.rad	3.89	4.22	4.5±0.3
Natural energy spread	9.8×10^{-4}	11.1×10^{-4}	$(10\pm2)\times10^{-4}$
Momentum compaction factor	4.27×10^{-4}	4.2×10^{-4}	$(4.0\pm0.5)\times10^{-4}$
Energy loss per turn / MeV	1.44	1.70	1.8±0.2
Damping time (H, V, S) / ms	7.05, 7.02, 3.51	5.98, 5.94, 2.96	6.0, 6.0, ---
Synchrotron tune	0.0076	0.0074	0.0072±0.0002
Bunch length	3.8 mm (zero-current)	4~8 mm(zero-current)	------ ~50 ps (200mA, no HC)

Beam Manipulations

◆ Closed Orbit Deviations (COD) and Feedback

- Caused by all the dipole field errors (tilts in Dipoles, misalignments in Multipoles, imperfections in IDs…)

$$z(s) = \frac{\sqrt{\beta_s}}{2\sin\pi\nu}\sum_{i=1}^{N}\sqrt{\beta_{s_i}}\theta_i\cos(\pi\nu - |\psi_s - \psi_{s_i}|)$$

- Severe CODs will make restoration of lattice perfermance difficult, and create significant defference between optical path in beamlines and electron path.

- Small dipole corrector are used to correct COD.

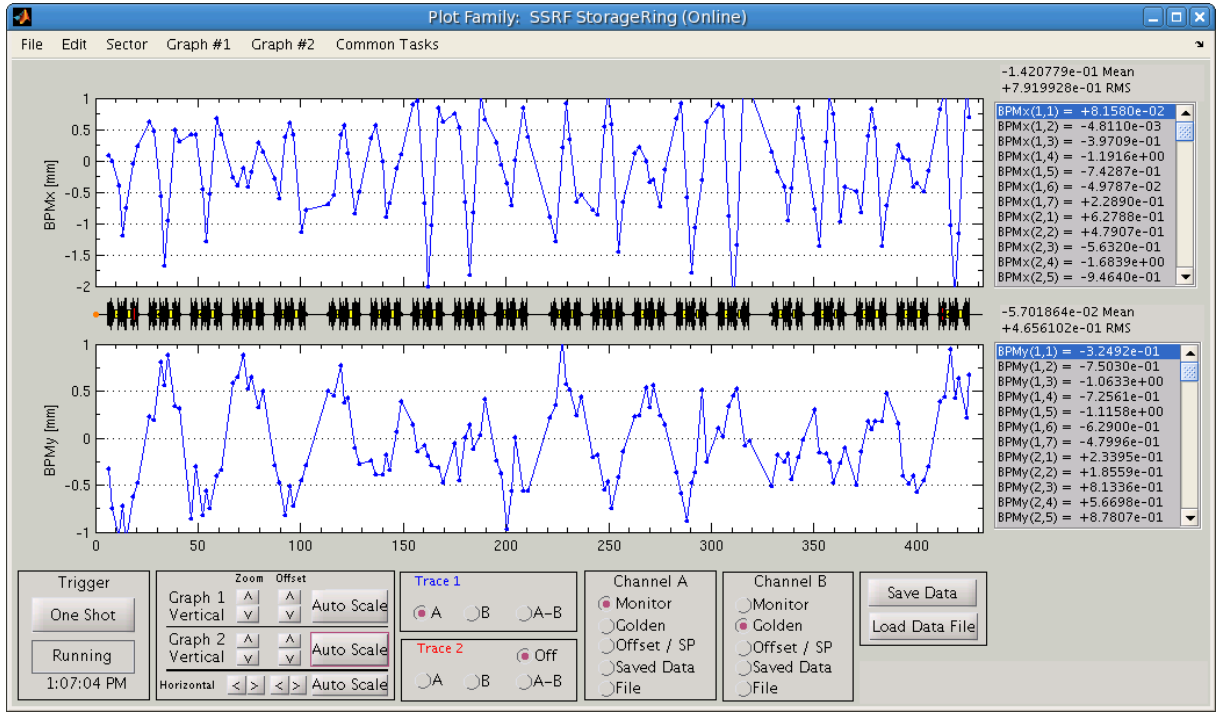

➢ COD correction

- SSRF: 80 slow correctors+140 BPMs
- Algorithm: Steepest Descent Method + Singular Value Decomposition (SVD)

$$Z = (z_1, z_2, \ldots z_m), \Theta = (\theta_1, \theta_2, \ldots \theta_n)$$

$$R_{i,j} = \partial\, z_i / \partial\, \theta_j$$

$$\Theta_{new} = \Theta_0 - R^{-1} Z_0$$

- In most cases the RM is not invertible, so SVD method is applied to provide a quasi-inversed matrix of RM.

$$R = USV^T$$

$$\Theta_{new} = \Theta_0 - (V(:, 1{:}N_s) S(1{:}N_s, 1{:}N_s)^{-1} U(:, 1{:}N_s)^T) Z_0$$

- The best CODs in the SSRF storage ring are about **50~80μm** (RMS along the ring) after correction.

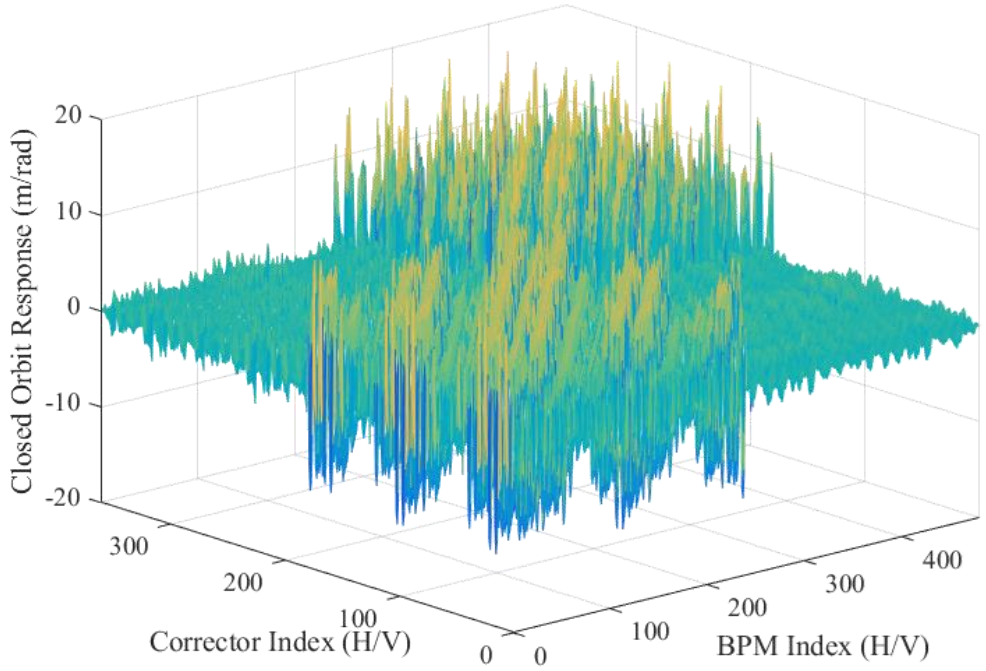

➢ Closed Orbit Stability

- Severe vibrations of COD will reduce the flux of beamlines, and cause data error in scientific experiments.

- Orbit instability originates from errors in measurement system (BPM noises) and vibrations of magnetic field .

  - Ground shrinkage and expansion with temperature (<1e-3Hz)
  - Drift in power supplies (low frequency <1e-2Hz)
  - ID adjustments (low frequency ~0.1Hz)
  - Higher frequency ripples in power supplies (>10Hz)
  - Turbulence in cooling system (>10Hz)
  - High frequency vibrations from outside of the facility (Traffic)

- Orbit feedback system in SSRF

  - Soft orbit feedback (Combined f_{RF}) + Fast orbit feedback
  - 80 slow correctors + 40 fast correctors for each plane

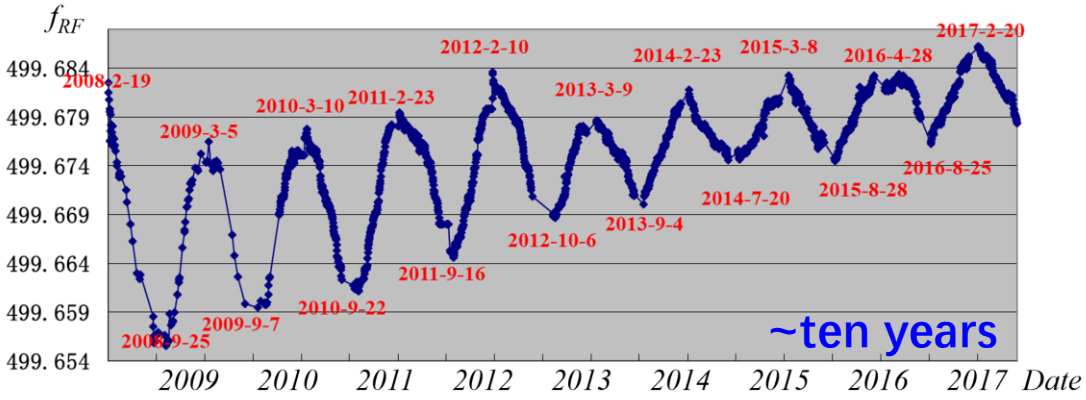

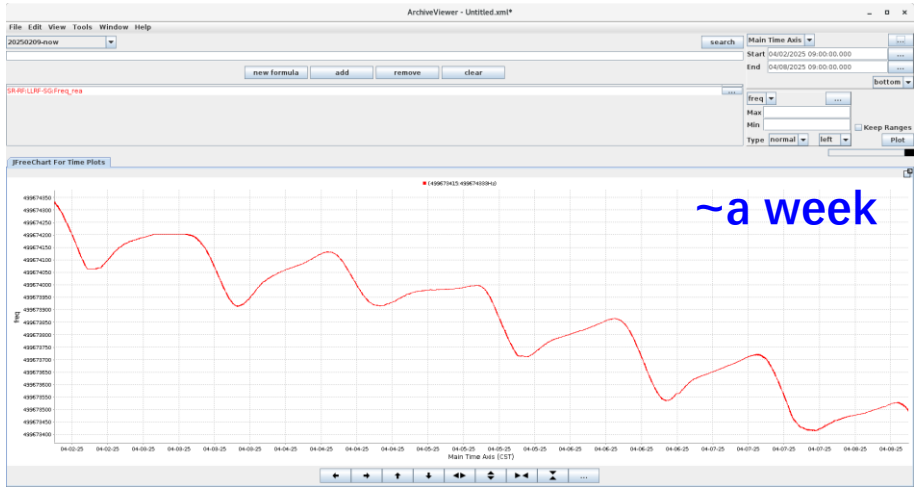

RF frequency variation with time/date

- Classic specification in orbit stability: RMS~10%$\sigma_{x,y}$, ~1μm for SSRF.
- Successfully suppress of COD instability less than 100 Hz (cut down by eddy current in vacuume vessel and BPM noise).
- RMS orbit stability reached the level of sub-μm (~500nm) in SSRF.

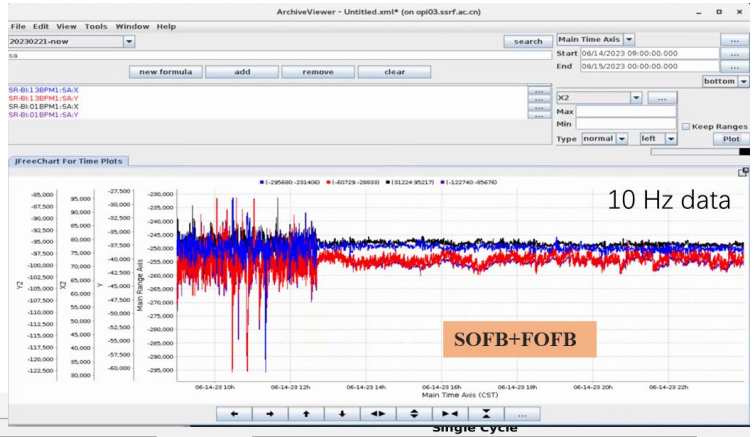

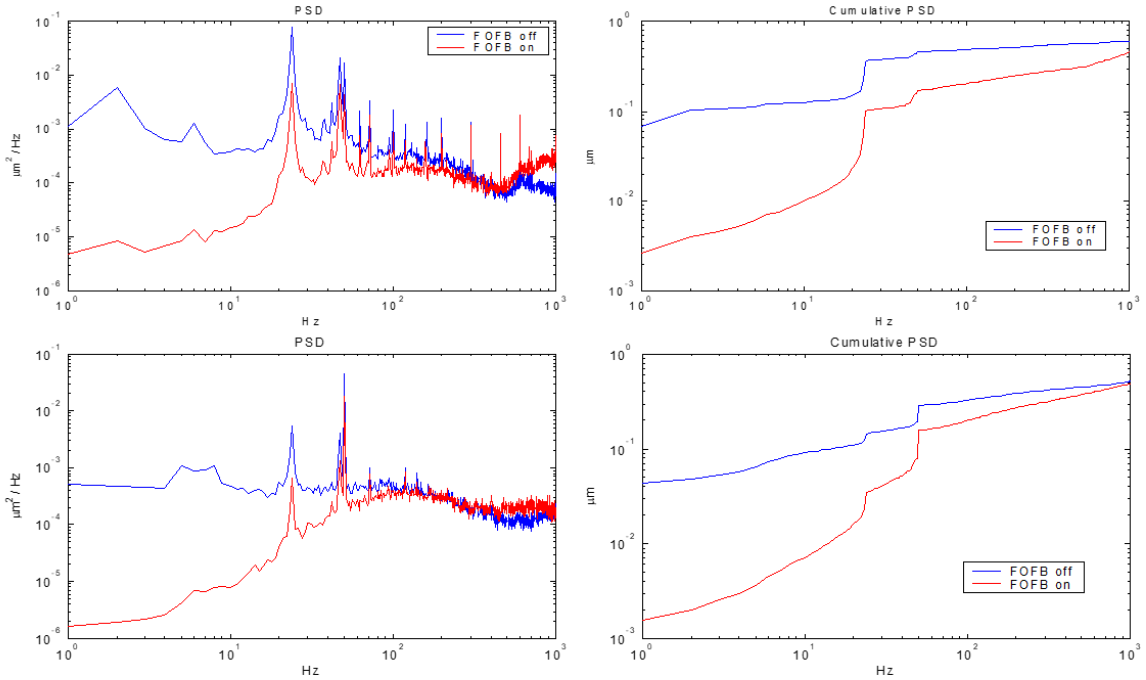

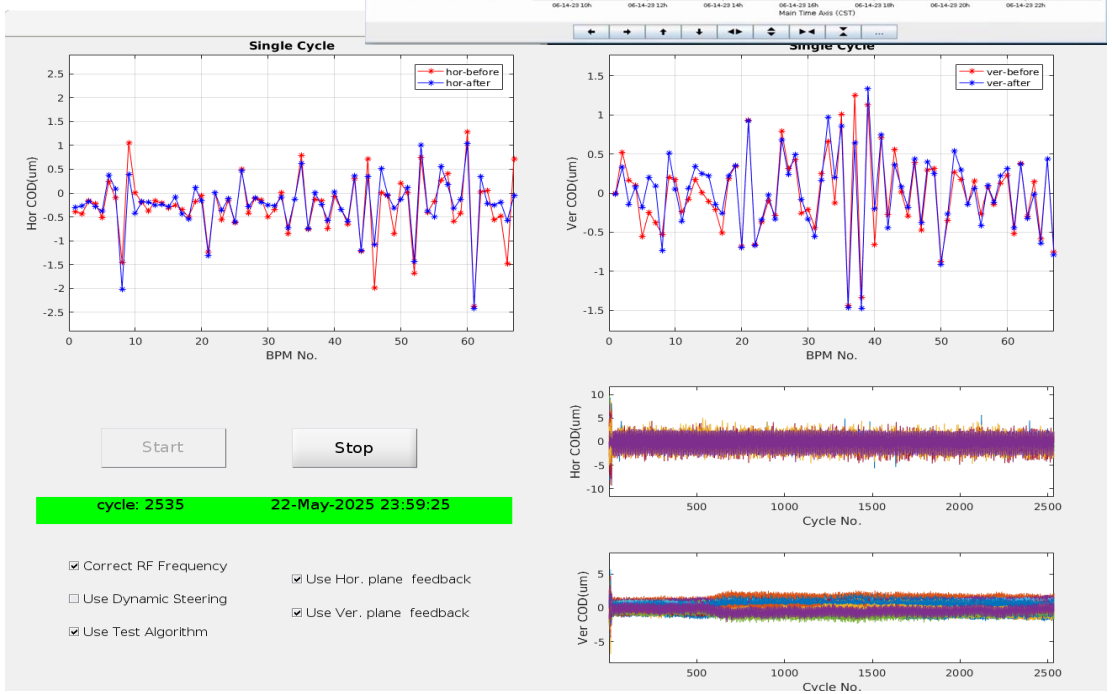

◆ Beam Optics Correction and Feedback

- ➢ Beam optics distorations caused by quadrupole errors make the optimal performance inavailable for users' experiments. So, we need to regularly correct the beam optics. Or, if we can, implemente optics feedback.
- Beta-beatings: beta function divation ratio from design one.
- ➢ Linear Optics from Closed Orbit response matrix (LOCO):

$$R_{jk} = \frac{\sqrt{\beta_j \beta_k}}{2\sin(\pi\upsilon)} \cos\left(\pi\upsilon - \left|\psi_j - \psi_k\right|\right) \qquad \chi^2 = \sum_{j,k} \frac{\left(R_{Mode,j,k} - R_{Meas,j,k}\right)^2}{\sigma_j^2}$$

- Minimizing the χ^2 by adjusting quadrupole gradients, we can get a lattice modelling the operating storage ring. (Decent method: Levenberg-Marquardt algorithm)

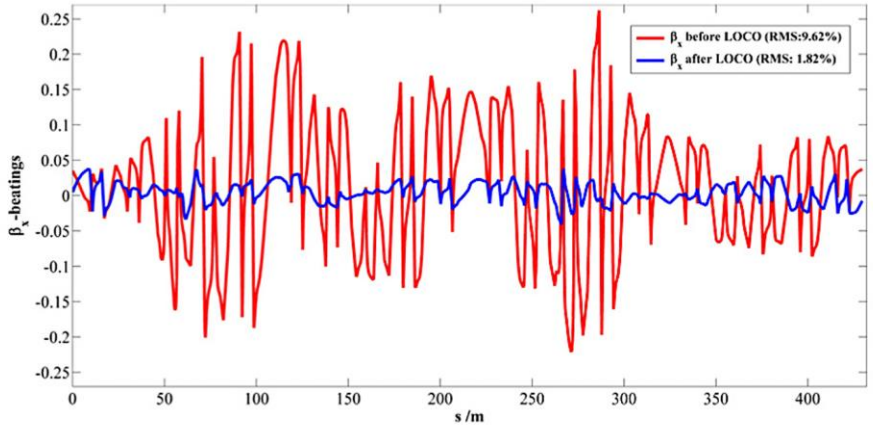

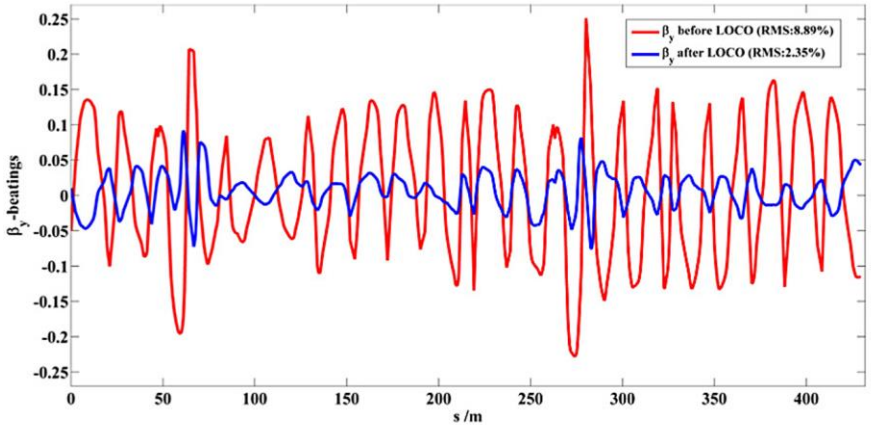

➢ Beam Optics Feedback with Neural Network

- It works well to correct the beam optics with LOCO and MIA. However, these methods need strong drive to the electron beam, and cannot implement optics feedback during routine operation.

- Beam optics feedback system applying deep learning method with the input of TBT data and output of quadrupole gradients.

- Process:

  - Sampling (get beam spectrum in every BPM in the ring)
  - Phase advance prediction from beam spectrum with Convolutional Neural Network (CNN)
  - Gradient prediction from phase advace with Constrained Fitting Neural Network (CFNN)
  - Correct or feedback the beam optics if necessary.

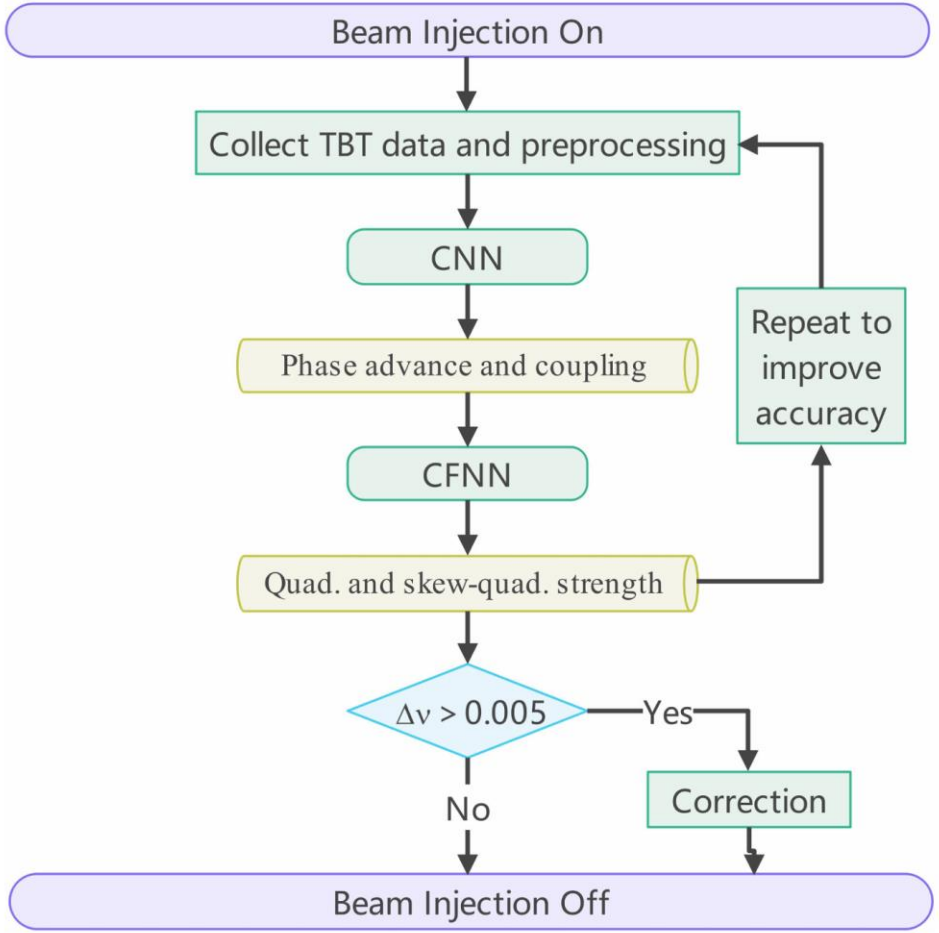

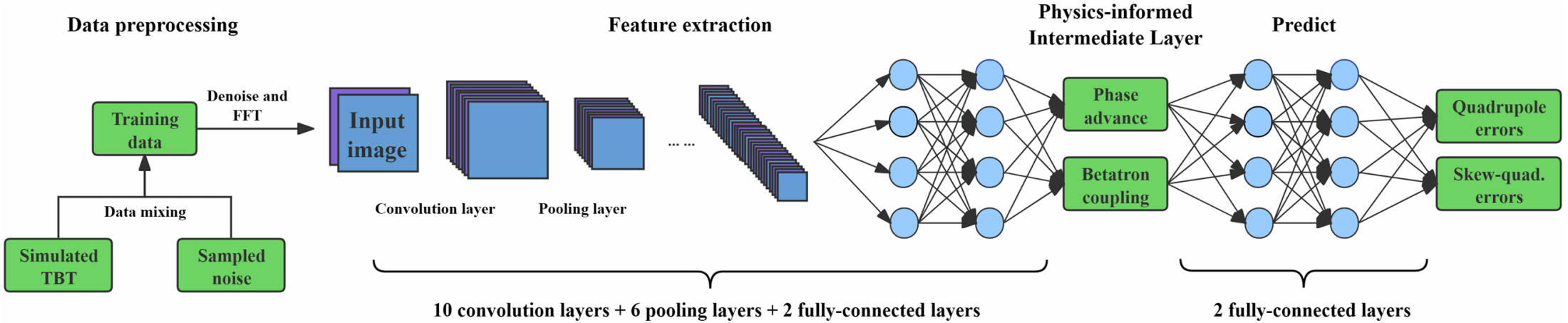

FIG. 8. Schematic diagram of the complete network architecture, including mixed training dataset generation, data denoise and preprocessing, a CNN for feature extraction, and fully-connected layers for quadrupole and skew-quadrupole error prediction. The phase advance and betatron coupling parameters output by the CNN are treated as a physics-informed intermediate layer and integrated into the model training process.

DOI: https://doi.org/10.1103/l1gf-558m

- Test-I:

- Test in machine study time
- Active error settings in Quadrupole PSs

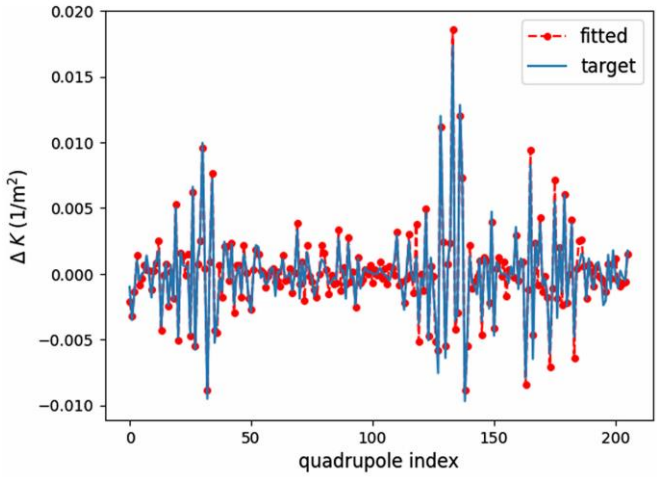

- Comparision with LOCO results

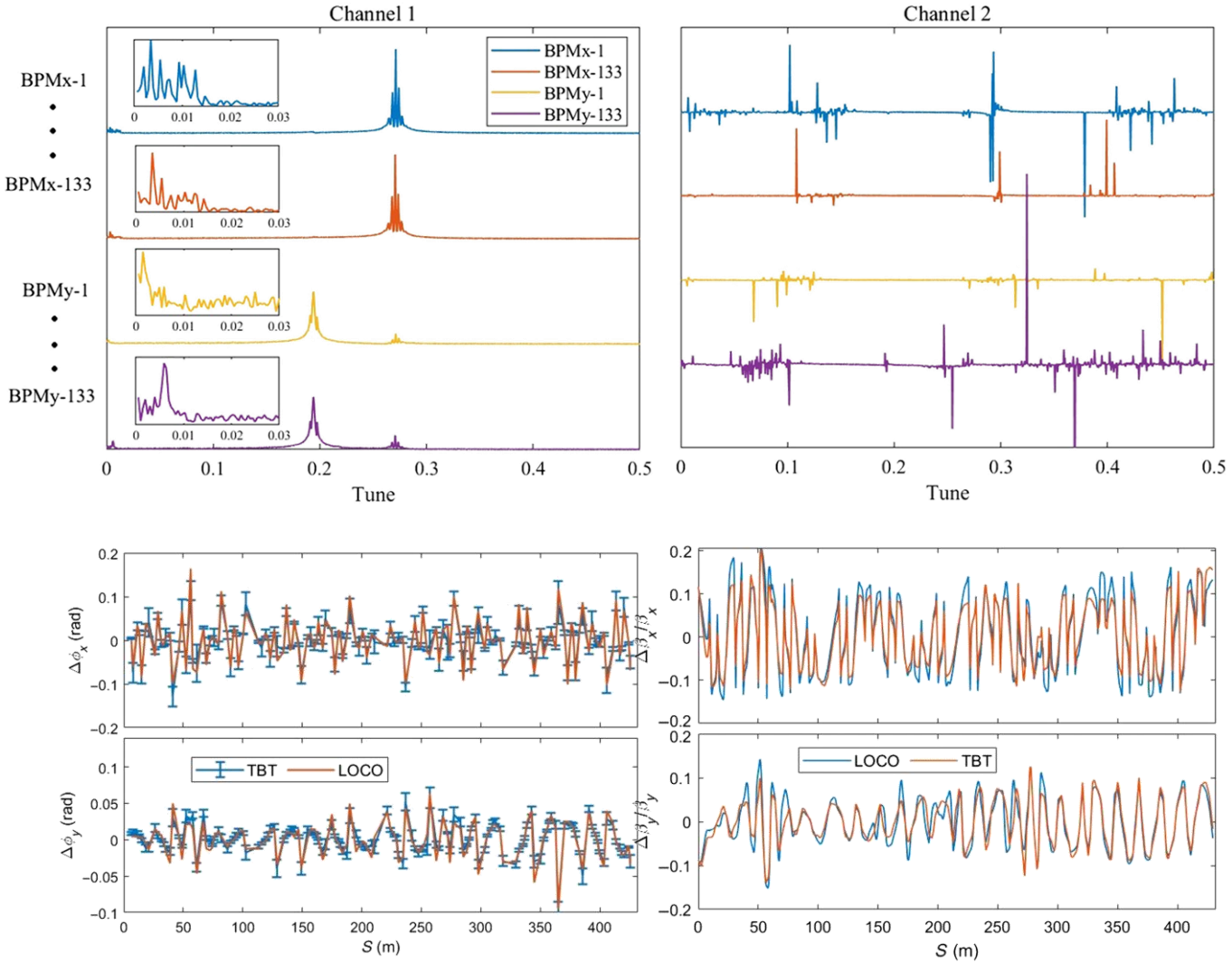

- Test-II:

- Test in TOPUP (without double-check by LOCO)
- Active error settings in PSs or change in EPUs

- This technique enables continuous monitoring and correction during each injection cycle.

- It had neither over-corrected beam optics nor over-predicted quadrupole PSs.

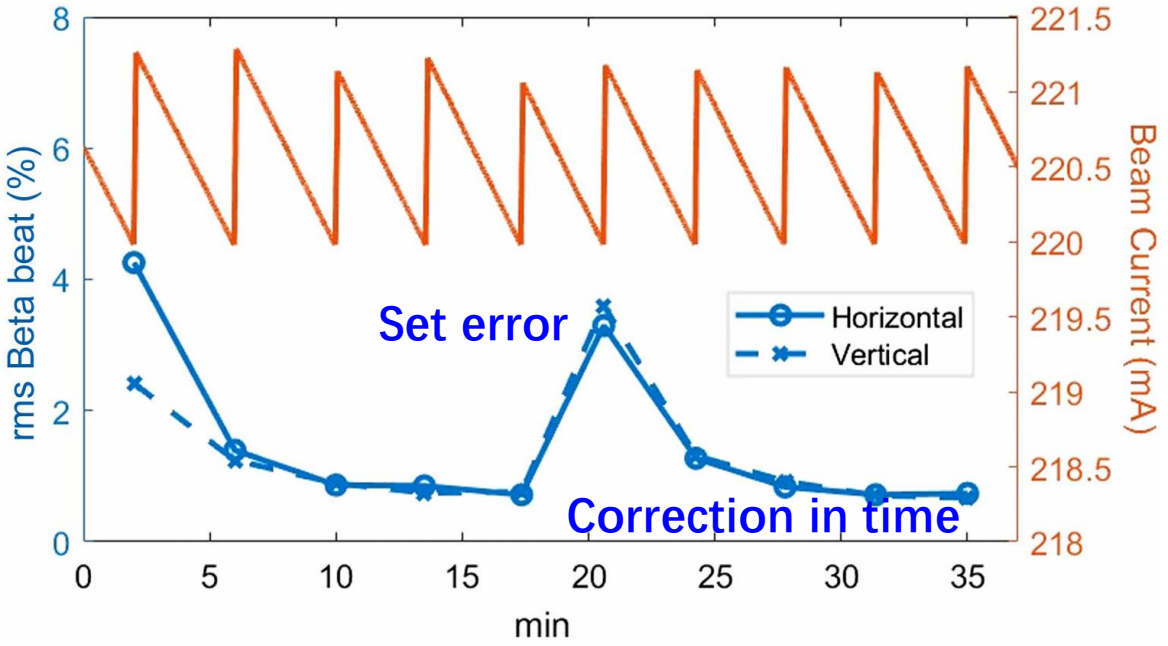

- Discussions

- This feedback technique can be applied in the storage ring with a few injection disturbation (~100μm in our case), while not available in Pulsed Multipole or SWAP-OUT injection.
- A dedicated kicker is helpful in PM and SO injection. It can drive the electron beam every tens of munites.
- How do we reduce the required amplitude of the residual beam oscilation?

◆ Filling Patterns

- 500-bunch-train filling
- 4 bunch-trains filling: 4×125, 200 mA
  Std (uniformity) better than 1%
  Developed to suppress fast ion instability
- Hybrid filling: 1×500+1, 180+20 mA
  Purity of the single bunch better than 1%
  less than 10% user time, at present
  Developed for fast-imaging experiments

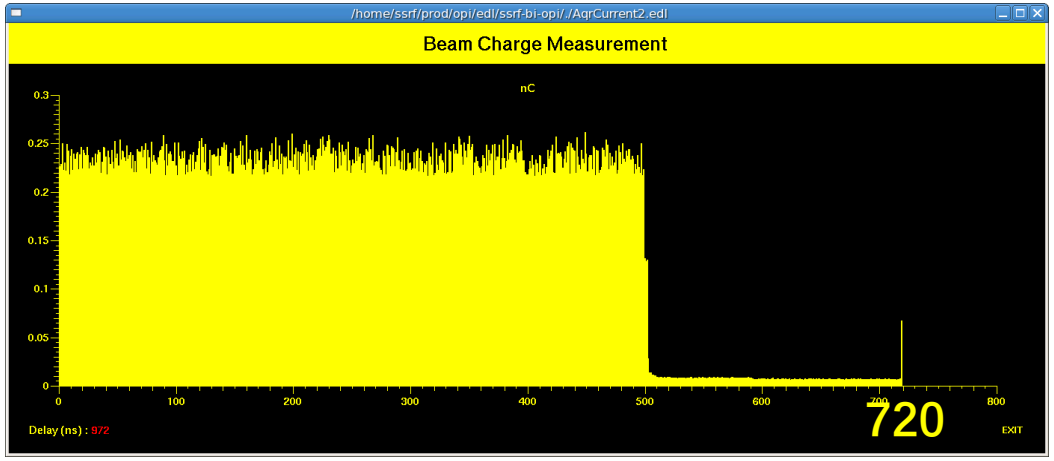

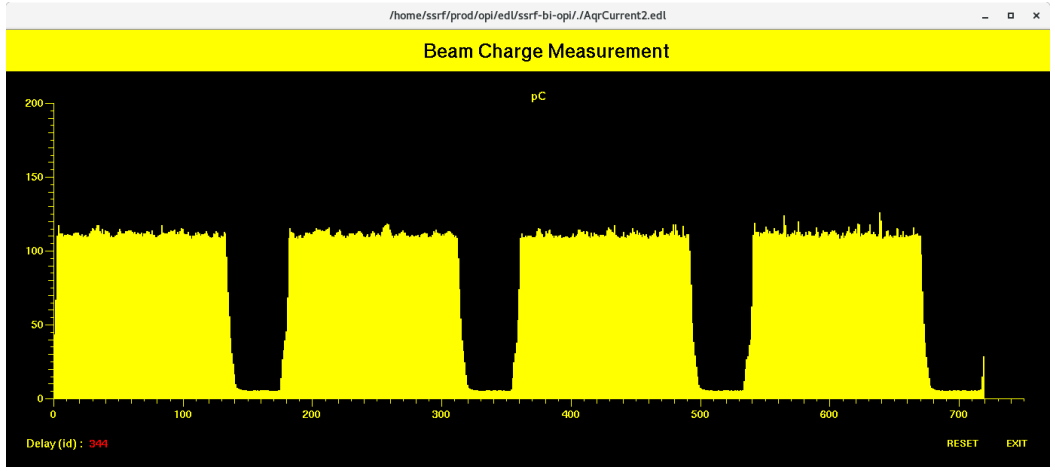

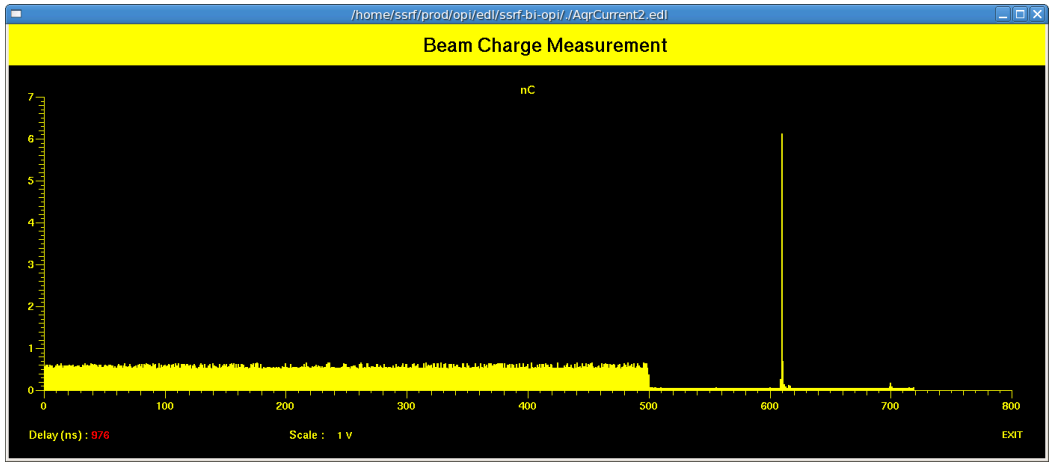

Outline

- The Way to the 3rd GLS
- Progress in the 3rd GLS
- Overview of SSRF
- Beam Dynamics in SSRF
- **Summary**

Summary

- The synchrotron radiation light sources have gone through four generations of development. The 3rd GLSs are featured by low-emittance C-G lattice, high fulx and brilliance radiation mainly from IDs, large capacity for beamlines.

- More than twenty 3rd-GLS facilities are in routine operation all over the world. Most of all the facilities are exploring and seeking for upgrade plans/proposals that apply MBA lattice to reduce the emittance down to X-ray diffraction limits.

- To reach low emittance in DBA/TBA lattice, nonliear optimization based on harmonic sextupoles and techniques/algorithms, such as FMA and MOGA, were developed in the 3rd GLSs. In terms of stability, TOPUP injection, bunch lengthening with harmonic cavity became standard operation methods.

- SSRF, a 3rd generation medium-energy light source, has been operated for sixteen years. 34 beamlines and 46 experimental stations are serving the scientific researches and industrial applications.


Thanks for
your attention!